

A fusion learning method to subgroup analysis for longitudinal trajectories

Mingming Liu¹, Jing Yang², Yushi Liu³, Bochao Jia³, Yun-Fei Chen³, Luna Sun³, Shujie Ma¹, and the Alzheimer's Disease Neuroimaging Initiative⁴

¹Department of Statistics, University of California at Riverside, Riverside, CA, U.S.A

²Key Laboratory of Computing and Stochastic Mathematics (Ministry of Education), College of Mathematics and Statistics, Hunan Normal University, Changsha, China

³Global Statistical Science, Eli Lilly and Company, Indianapolis, IN, U.S.A

Abstract

Uncovering the heterogeneity in the disease progression of Alzheimer's is a key factor to disease understanding and treatment development, so that interventions can be tailored to target the subgroups that will benefit most from the treatment, which is an important goal of precision medicine. However, in practice, one top methodological challenge hindering the heterogeneity investigation is that the true subgroup membership of each individual is often unknown. In this paper, we aim to identify latent subgroups of individuals who share a common disorder progress over time, to predict latent subgroup memberships, and to estimate and infer the heterogeneous trajectories among the subgroups. To achieve these goals, we propose a nonparametric fusion learning method that can automatically identify subgroups and recover the heterogeneous trajectories, which are represented by subject-specific unknown functions. We approximate the unknown functions by B-splines, and apply a concave fusion penalization method that can merge the estimated functions together for the subjects belonging to the same subgroup. The resulting estimator of the disease trajectory of each subgroup is supported by an asymptotic distribution. It provides a sound theoretical basis for further conducting statistical inference in subgroup analysis. Our method is applied to a longitudinal Alzheimer's Disease data set.

Key Words: B-spline; Concave penalty; Heterogeneity; Longitudinal trajectory; Precision medicine; Subgroup analysis

Mingming Liu and Jing Yang are joint first authors. Correspondence should be addressed to Shujie Ma. Email: shujie.ma@ucr.edu.

1 Introduction

Alzheimer’s disease (AD) is the leading cause of dementia for adults. It is a progressive disease that worsens over time. Patients with AD show symptoms of memory loss, mental decline, delusion and so forth as the disease progresses. The progression of AD varies from person to person, and patients with AD have experienced it in different ways. The lack of a good understanding of the heterogeneity in the disease progression through the population is a key reason for failures of disease-modifying treatments for AD. As a result, very little progress has been made for the AD treatment development since 2003 (Yiannopoulou et al., 2019). To overcome this difficulty, one has to first understand the heterogeneity in the disease trajectories, so that interventions can be tailored to target the subgroups that will benefit most from the treatment, which is an important goal of precision medicine. The progression of AD is often measured by cognitive scores at multiple time points, resulting in a collection of longitudinal data. One major methodological challenge hindering the heterogeneity investigation is that the true subgroup membership of each individual is often unknown.

The growth mixture modeling (GMM) method (Fraley and Raftery, 2002; Song et al., 2007; Jung and Wickrama, 2008; McNicholas, 2010) has been popularly used for the identification and prediction of latent subpopulations for longitudinal data. This method requires to specify the underlying distribution of the data, which is often hard to obtain for longitudinal data, because of their complex structure. The k-means algorithm (Hartigan and Wong, 1979) is another popular clustering method. It divides the data into subgroups based on the distances between measurement vectors of subjects. It is difficult to apply this method to cluster functional curves, especially arising from longitudinal data with missing measurements. Moreover, both GMM and k-means methods need to pre-specify the number of subgroups, which is often unknown in practice, and thus introduces additional complications in the estimation procedure.

To overcome these challenges, we apply the fusion learning method proposed in Ma and Huang (2017); Ma et al. (2019) to conduct subgroup analysis for longitudinal trajectories of the AD data. This semi-supervised machine learning method applies concave penalty functions to pairwise differences of clinical outcomes or unknown treatment coefficients in a regression model. It can

automatically identify memberships from latent subgroups and estimate the number of subgroups simultaneously without specifying the underlying distribution. [Ma and Huang \(2017\)](#); [Ma et al. \(2019\)](#) proposed this fusion learning method for the cross-sectional data with independent subjects observed at one time point. In this paper, we extend it to the longitudinal data with balanced or unbalanced repeated measures. However, it requires a different estimation strategy from the one considered in [Ma and Huang \(2017\)](#); [Ma et al. \(2019\)](#) given that nonlinear disease trajectories and correlated repeated measures are involved in the problem.

To cluster the AD patients based on their cognitive scores observed over time, we consider a subject-specific nonparametric regression model, in which the heterogeneity can be driven by observed or unobserved latent covariates. More specifically, we model each patient’s cognitive scores through an unknown functional curve of time. We approximate each curve by B-splines ([De Boor, 2001](#); [Liu and Yang, 2010](#); [Xue and Liang, 2013](#); [Ma, 2014](#)), and then apply pairwise fusion penalties to the spline coefficients, so that patients with similar disease trajectories can be automatically clustered into the same homogeneous subgroup. As a result, patients in the same identified subgroup share the same disease progressive curve. We use an alternating direction method of multipliers (ADMM) algorithm ([Boyd et al., 2011](#)) that has a good convergence property to solve the optimization problem. Different from the GMM method, our method does not require to pre-specify the number of subgroup, nor does it need to provide the underlying distribution of the data. Instead, our estimation procedure only involves a working correlation matrix ([Liang and Zeger, 1986](#); [Wang et al., 2005](#); [Ma, 2012](#); [Ma et al., 2013](#)) for the repeated measures of each subject, and the resulting estimator of the functional curve for each subgroup is robust to the specification of the correlation matrix, i.e., it is still a consistent estimator even if the working correlation matrix is mis-specified.

The rest of this article is organized as follows. Section 2 describes the proposed model. Section 3 introduces the model estimation procedure using concave fusion penalization method. In Section 4, we establish the theoretical properties of the proposed estimators. Simulation studies are presented in Section 5. Section 6 illustrates the application of the proposed method via Alzheimer’s disease data. Discussions are provided in the last section. The related computation procedure and technical

proof are included in the Appendix.

2 Model

Suppose the data consists of:

$$\{(Y_{ij}, t_{ij}), 1 \leq i \leq n, 1 \leq j \leq m_i\}, \quad (2.1)$$

where $\{t_{ij}, j = 1, \dots, m_i\}$ are the distinct time points that the measurements of the i th subject are taken and Y_{ij} is the observed response for the i th subject at time t_{ij} . Our goal is to understand how the change of trajectories may differ across individual subjects.

To study the longitudinal trajectories of $Y_i(t)$, we consider the subject-specific nonparametric regression model:

$$Y_i(t) = \beta_i(t) + \varepsilon_i(t), \quad i = 1, \dots, n, \quad (2.2)$$

where $\beta_i(t)$ are the unknown smooth functions of t . We assume that the error terms $\varepsilon_i(t)$ satisfy $E\{\varepsilon_i(t)\} = 0$ and $\text{Cov}(\varepsilon_i(t), \varepsilon_{i'}(s)) = \gamma(t, s)I\{i = i'\}$. Under this model, the trajectory of the i th subject over time is represented by the subject-specific unknown function $\beta_i(t)$. Due to the heterogeneity of the trajectories, we assume $\beta_i(t)$ in (2.2) arise from K different groups with $K \geq 1$. To be specific, we have $\beta_i(t) = \alpha_k(t)$ for all $i \in \mathcal{G}_k$, where $\mathcal{G} = (\mathcal{G}_1, \dots, \mathcal{G}_K)$ is a mutually exclusive partition of $\{1, \dots, n\}$ and $\alpha_k(t)$ is the common function for all the $\beta_i(t)$'s from group \mathcal{G}_k .

Then the repeated measurements in (2.1) can be regarded as a random sample from model (2.2) with the form,

$$Y_{ij} = \beta_i(t_{ij}) + \varepsilon_{ij}, \quad (2.3)$$

where $Y_{ij} = Y_i(t_{ij})$, $\varepsilon_{ij} = \varepsilon_i(t_{ij})$ and $\beta_i(t_{ij}) = \alpha_k(t_{ij})$ if $i \in \mathcal{G}_k$.

No matter the number of subgroups K is known or unknown, it is much smaller than the sample size n .

3 Estimation

In order to identify the subgroups of the heterogeneous trajectories, we first approximate the nonparametric functions $\beta_i(\cdot)$'s in (2.3) by B-splines.

To introduce B-splines, let $a = t_0 < t_1 < \dots < t_{J_n} < t_{J_n+1} = b$ be a sequence of J_n interior knots, where J_n increases with the sample size n . Interval $[a, b]$ will be partitioned into $J_n + 1$ subintervals $I_s = [t_s, t_{s+1})$, $s = 0, \dots, J_n - 1$, and $I_{J_n} = [t_{J_n}, 1]$. Denote by G the space consisting of functions that are polynomials of degree $(q - 1)$ on each subinterval and $q - 2$ times continuously differentiable for $q \geq 2$, where q is the spline order. Then, $\beta_i(t)$ can be approximated well by the spline functions,

$$\beta_i(t_{ij}) \approx \sum_{l=1}^d \gamma_{il} B_l(t_{ij}) = \mathbf{B}_{ij}^T \boldsymbol{\gamma}_i, \quad i = 1, \dots, n, \quad j = 1, \dots, m_i, \quad (3.1)$$

where $\{B_l(\cdot), l = 1, \dots, d\}$ is the normalized B-spline basis of the space (De Boor, 2001), the number of basis functions is $d = J_n + q$, $\mathbf{B}_{ij} = (B_1(t_{ij}), \dots, B_d(t_{ij}))^T$ and $\boldsymbol{\gamma}_i = (\gamma_{i1}, \dots, \gamma_{id})^T$ are $d \times 1$ vectors. In this case, the trajectory heterogeneity that represented by $\beta_i(t)$, is reflected on the B-spline coefficient $\boldsymbol{\gamma}_i$. Therefore, our goal can be transformed into identifying the subgroups based on the $\boldsymbol{\gamma}_i$'s.

For simplicity, let $\mathbf{Y}_i = (Y_{i1}, \dots, Y_{im_i})^T$, $\boldsymbol{\varepsilon}_i = (\varepsilon_{i1}, \dots, \varepsilon_{im_i})^T$ and $\mathbf{X}_i = (\mathbf{B}_{i1}, \dots, \mathbf{B}_{im_i})^T$. Given (3.1), for each i , model (2.3) can be written in matrix notation as

$$\mathbf{Y}_i \approx \mathbf{X}_i \boldsymbol{\gamma}_i + \boldsymbol{\varepsilon}_i, \quad i = 1, \dots, n, \quad (3.2)$$

Let $\boldsymbol{\Sigma}_i$ and \mathbf{V}_i be the true and assumed working covariance of \mathbf{Y}_i , where $\mathbf{V}_i = \mathbf{A}_i^{1/2} \mathbf{R}_i \mathbf{A}_i^{1/2}$. Here, \mathbf{A}_i is a $m_i \times m_i$ diagonal matrix containing the marginal variances of Y_{ij} , and \mathbf{R}_i is the corresponding working correlation matrix. Throughout, we assume that \mathbf{V}_i depends on a nuisance finite dimensional parameter vector $\tilde{\boldsymbol{\theta}}$.

Following Ma et al. (2019), we utilize a fusion learning approach with a concave penalty to estimate model (3.2). The objective function is constructed as:

$$Q_n(\boldsymbol{\gamma}; \lambda) = \frac{1}{2} \sum_{i=1}^n (\mathbf{Y}_i - \mathbf{X}_i \boldsymbol{\gamma}_i)^T \mathbf{V}_i^{-1} (\mathbf{Y}_i - \mathbf{X}_i \boldsymbol{\gamma}_i) + \sum_{1 \leq i < j \leq n} p(\|\boldsymbol{\gamma}_i - \boldsymbol{\gamma}_j\|_2, \lambda), \quad (3.3)$$

where $\|\cdot\|_2$ represents the L_2 norm with $\|\mathbf{a}\|_2 = (\sum a_i^2)^{1/2}$, $\boldsymbol{\gamma} = (\boldsymbol{\gamma}_1^T, \dots, \boldsymbol{\gamma}_n^T)^T$ and $p(\cdot, \lambda)$ is a concave penalty function with a tuning parameter $\lambda \geq 0$. For a given $\lambda > 0$, define

$$\hat{\boldsymbol{\gamma}}(\lambda) = \arg \min_{\boldsymbol{\gamma}} Q_n(\boldsymbol{\gamma}; \lambda). \quad (3.4)$$

When λ is large enough, the penalty shrinks some pairs of $\|\gamma_i - \gamma_j\|_2$ to zero. Based on this fact, we can partition the heterogeneous trajectories into subgroups. To select the optimal tuning parameter $\hat{\lambda}$, we consider two situations. When the actual number of subgroups K is known, we choose a λ value on the solution path such that the corresponding estimated number of subgroups equalling true number of subgroups. For the unknown situation, $\hat{\lambda}$ is selected on a data-driven procedure such as BIC or the Calinski-Harabaz index. For convenience, we write $\hat{\gamma}(\hat{\lambda}) \equiv \hat{\gamma}$. Let $\{\hat{\gamma}_{(1)}, \dots, \hat{\gamma}_{(\hat{K})}\}$ be the unique values of $\hat{\gamma}$ and $\{\hat{\alpha}_1(t), \dots, \hat{\alpha}_{\hat{K}}(t)\}$ be the corresponding functions. Similarly, we write $\{\hat{\alpha}_1, \dots, \hat{\alpha}_{\hat{K}}\} \equiv \{\hat{\alpha}_1(t), \dots, \hat{\alpha}_{\hat{K}}(t)\}$, $\{\hat{\beta}_1, \dots, \hat{\beta}_n\} \equiv \{\hat{\beta}_1(t), \dots, \hat{\beta}_n(t)\}$, $\{\alpha_1, \dots, \alpha_K\} \equiv \{\alpha_1(t), \dots, \alpha_K(t)\}$ and $\{\beta_1, \dots, \beta_n\} \equiv \{\beta_1(t), \dots, \beta_n(t)\}$. Then, given (3.1), in the k th subgroup ($1 \leq k \leq \hat{K}$), we have $\hat{\mathcal{G}}_k = \left\{ i : \hat{\beta}_i = \hat{\alpha}_k \approx \mathbf{B}_{ij}^T \hat{\gamma}_{(k)}, 1 \leq i \leq n \right\}$.

An appropriate selection of the penalty is very critical to the model estimation. Instead of choosing lasso penalty $p_\tau(t, \lambda) = \lambda |t|$ (Tibshirani, 1996), which results in biased estimates due to the over-shrinkage of large coefficients, we use the minimax concave penalty (MCP) (Zhang, 2010) by inducing nearly unbiased estimators with the form

$$p_\tau(t, \lambda) = \lambda \int_0^{|t|} (1 - x/(\tau\lambda))_+ dx, \quad \tau > 1,$$

where τ is a parameter controlling the concavity of the penalty function. Moreover, it is more aggressive in enforcing a sparser solution. Consequently, MCP is a more desirable choice. The details for computational procedure using ADMM algorithm for a given value of λ are provided in the Appendix.

Another problem is how to choose the working covariance matrix \mathbf{V}_i . Here we consider an unequally spaced AR(1) structure for the working covariance matrix \mathbf{V}_i , such that $V_i(t, s) = \sigma^2 \rho^{\kappa|t-s|}$, where $\kappa = \frac{1}{|t_{(1)} - t_{(2)}|}$ with $t_{(1)}, t_{(2)}$ being the first two time points. Note that our estimator of the functional curve for each subgroup is consistent even if the working covariance matrix is misspecified, i.e., $\mathbf{V}_i \neq \mathbf{\Sigma}_i$, where $\mathbf{\Sigma}_i$ is the true covariance matrix. First, we estimate σ^2 by taking the mean of the estimated variance $\hat{\sigma}_i^2$, $i = 1, \dots, n$, where $\hat{\sigma}_i^2$ is calculated within subject by using ordinary least squares (OLS) residuals. Due to the fact that these residuals may be small and thus underestimate the true errors, we modify these residuals by replacing $\hat{\varepsilon}_{ij}$ with $\hat{\varepsilon}_{ij}^* = \hat{\varepsilon}_{ij}/(1 - h_{ij})$, where h_{ij} is the j th diagonal element of the projection matrix \mathbf{H}_i for subject i . This modification

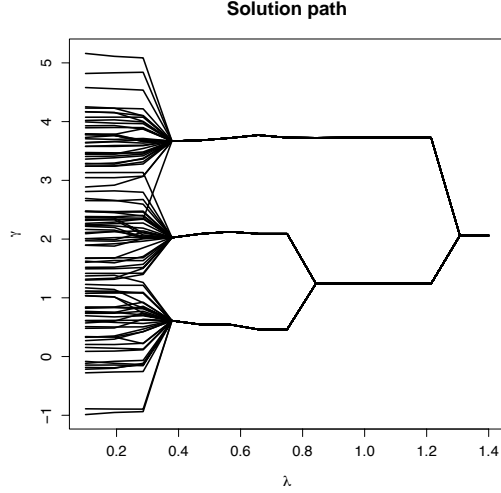


Fig. 1: Solution path for $(\hat{\gamma}_{31}(\lambda), \dots, \hat{\gamma}_{3n}(\lambda))$ against λ with $n = 100$, $T = 20$ for balanced data of Middle case from Three Subgroup Example in Section 5.

is suggested by [MacKinnon and White \(1985\)](#). Given (3.2), we have $\mathbf{H}_i = \mathbf{X}_i(\mathbf{X}_i^T \mathbf{X}_i)^{-1} \mathbf{X}_i^T$. Next, we estimate correlation ρ by taking the average of the estimated correlation between the two adjacent time points, in which we only consider the adjacent time points having the scaled distance equalling 1, i.e. $\kappa |t - s| = 1$. Accordingly, \mathbf{V}_i can be obtained.

Figure 1 illustrates the solution path for the estimates of B-spline coefficients $(\hat{\gamma}_{31}(\lambda), \dots, \hat{\gamma}_{3n}(\lambda))$ against λ , which is computed on a grid of λ values in interval $[\lambda_{\min}, \lambda_{\max}]$. More details about the solution path are presented in Subsection A.1.1. From Figure 1, we observe that when λ is very small, too many subgroups are identified. With λ value increasing, the estimated number of subgroups decreases, then becomes to 1 for a large λ value. If the actual number of subgroups is given (here $K = 3$), based on the solution path, we can select a λ between 0.6 and 0.8 as the tuning parameter, where \hat{K} equals the true number of subgroups; otherwise, BIC or the Calinski-Harabaz index is used to decide the optimal tuning parameter.

4 Theoretical properties

In this section, we establish the theoretical properties of the proposed estimators. We first introduce some notations. Let $\boldsymbol{\alpha} = (\alpha_1, \dots, \alpha_K)^T$ with α_k being the true function in the k th subgroup ($k = 1, \dots, K$) and $\boldsymbol{\beta} = (\beta_1, \dots, \beta_n)^T$ with β_i being the trajectory function of the i th subject. Define $\|\cdot\|_2$ as the usual 2-norm for functions or vectors, that is, $\|g\|_2^2 = \int_{\mathbb{T}} g(t)^2 dt$ for a square

integrable function g on \mathbb{T} , and $\|a\|_2^2 = \sum_{i=1}^n a_i^2$ for a n -dimensional vector $a = (a_1, \dots, a_n)^T$. For a vector valued function $\mathbf{g} = (g_1, \dots, g_L)^T$, denote $\|\mathbf{g}\|_2^2 = \sum_{l=1}^L \|g_l\|_2^2$. Let $m_{(n)} = \min_{1 \leq i \leq n} m_i$, $N_k = \sum_{i \in \mathcal{G}_k} m_i$, $N_0 = \min_{1 \leq k \leq K} N_k$ and $b = \min_{k \neq k'} \|\alpha_k - \alpha_{k'}\|_2$ be the minimum distance between smoothing functions α_k and $\alpha_{k'}$ from any two clusters.

4.1 Asymptotic properties

Definition. A random sequence $\{\xi_k, k \geq 1\}$ is said to be α -mixing if the α -mixing coefficient

$$\alpha(s) : \stackrel{\text{def}}{=} \sup_{k \geq 1} \sup\{|P(A \cap B) - P(A)P(B)| : A \in \mathcal{F}_{s+k}^\infty, B \in \mathcal{F}_1^k\}$$

converges to 0 as $s \rightarrow \infty$, where \mathcal{F}_a^b is the σ algebra generated by $\xi_a, \xi_{a+1}, \dots, \xi_b$.

Let \mathcal{H}_r be the collection of all functions on \mathbb{T} such that the q -th order derivative satisfies the Hölder condition of order $s > 0$ with $r \equiv q + s$. That is, there exists a positive constant C_0 such that for any function $\phi \in \mathcal{H}_r$,

$$|\phi^{(q)}(u_1) - \phi^{(q)}(u_2)| \leq C_0 |u_1 - u_2|^s$$

for any $u_1, u_2 \in \mathbb{T}$.

Given (3.3), we can write the objective function as

$$L_n(\boldsymbol{\gamma}) = \frac{1}{2}(\mathbf{Y} - \mathbf{X}\boldsymbol{\gamma})^T \mathbf{V}^{-1}(\mathbf{Y} - \mathbf{X}\boldsymbol{\gamma}) + \sum_{1 \leq i < j \leq n} P_\tau(\|\boldsymbol{\gamma}_i - \boldsymbol{\gamma}_j\|_2, \lambda),$$

where $\mathbf{Y} = (\mathbf{Y}_1, \dots, \mathbf{Y}_n)^T$, $\mathbf{X} = \text{diag}(\mathbf{X}_1, \dots, \mathbf{X}_n)$ and $\mathbf{V} = \text{diag}(\mathbf{V}_1, \dots, \mathbf{V}_n)$. Then, the estimator can be written as $\hat{\boldsymbol{\beta}} = \mathbf{X}\hat{\boldsymbol{\gamma}}$, where $\hat{\boldsymbol{\gamma}} = \arg \min_{\boldsymbol{\gamma}} L_n(\boldsymbol{\gamma})$.

Assume that the nonparametric functions $\beta_i(t) = \beta_j(t)$ if subjects i and j come from the same cluster group. The nonparametric function subspace $M_{\mathcal{G}}^\beta$ corresponding to the group partition is defined as

$$M_{\mathcal{G}}^\beta = \{\beta : \beta_i = \alpha_k, \beta_i \in \mathcal{H}_r, \text{ for any } i \in \mathcal{G}_k, 1 \leq k \leq K\}.$$

Accordingly, the subspace $M_{\mathcal{G}}^\gamma$ of the B-spline coefficients corresponding to the group partition is defined as

$$M_{\mathcal{G}}^\gamma = \left\{ \boldsymbol{\gamma} : \boldsymbol{\gamma}_i = \boldsymbol{\theta}_k, \boldsymbol{\gamma}_i \in R^d, \text{ for any } i \in \mathcal{G}_k, 1 \leq k \leq K \right\}.$$

Moreover, denote $\hat{\beta}^{or} = \mathbf{X}\hat{\gamma}^{or}$ as the oracle estimator, where $\hat{\gamma}^{or} = \arg \min_{\gamma \in M_{\mathcal{G}}^{\gamma}} (\mathbf{Y} - \mathbf{X}\gamma)^T \mathbf{V}^{-1} (\mathbf{Y} - \mathbf{X}\gamma)$.

Regularity conditions:

(C1) The observation time points t_{ij} , $i = 1, \dots, n$, $j = 1, \dots, m_i$ are chosen independently from a distribution $F(\cdot)$ with the density $f(\cdot)$. Moreover, the density function $f(t)$ is uniformly bounded away from 0 and infinity on its compact support \mathbb{T} . Without loss of generality, we assume $\mathbb{T} = [a, b]$.

(C2) There exists a positive constant M such that $E(\varepsilon(t)^4) \leq M$ for all $t \in \mathbb{T}$. In addition, the random sequence $\{\varepsilon_{ij}\}$ for each i satisfies α -mixing condition with the α -mixing coefficient satisfying $\alpha(s) \leq Cs^{-\alpha}$ for $\alpha > \frac{2+\kappa}{1-\kappa}$, where $0 < \kappa < 1$.

(C3) The functions $\beta_i(\cdot) \in \mathcal{H}_r$ for $i = 1, \dots, n$.

(C4) Let $a = t_0 < t_1 < \dots < t_{J_n} < t_{J_n+1} = b$ be a partition of $[a, b]$ into $J_n + 1$ subintervals, the knot sequences $\{t_l\}_{l=0}^{J_n+1}$ have bounded mesh ratio. That is, for some positive constant C

$$\frac{\max_{0 \leq l \leq J_n} |t_{l+1} - t_l|}{\min_{0 \leq l \leq J_n} |t_{l+1} - t_l|} \leq C.$$

(C5) The eigenvalues of $\Sigma = \text{diag}(\Sigma_1, \dots, \Sigma_n)$ and $\mathbf{V} = \text{diag}(\mathbf{V}_1, \dots, \mathbf{V}_n)$ are bounded away from zero to infinity.

Theorem 1 *Suppose conditions (C1)-(C5) hold, and for any fixed K , if $J_n = O(N_0^\varsigma)$ with $0 < \varsigma < 1$, the oracle estimator $\hat{\beta}^{or}$ satisfying $\|\hat{\beta}^{or} - \alpha\|_2^2 = O_p(J_n/N_0 + J_n^{-2r})$.*

Theorem 2 *Suppose conditions (C1)-(C5) hold, and for any fixed n , if there exist some constant $C > 0$ such that $Cb \geq \tau\lambda$ and $J_n = O(m_{(n)}^\varsigma)$ with $0 < \varsigma < 1$, then $\|\hat{\beta} - \beta\|_2^2 = O_p(J_n/m_{(n)} + J_n^{-2r})$.*

Theorem 3 *Assume that $\hat{\mathcal{G}}$ and \mathcal{G}_0 respectively be the estimated and true subgroup membership. Under the same conditions in Theorem 2, we have $P(\hat{\mathcal{G}} = \mathcal{G}_0) \rightarrow 1$ as $m_{(n)} \rightarrow \infty$.*

This theorem indicates that as long as the repeated measurements of each subject are sufficiently large, our proposed method can correctly identify the true sub-grouping structure with probability tending to 1. It follows from Theorems 1-3 that the proposed penalized estimators performs asymptotically equivalent to the oracle ones as $m_{(n)}$ approaching to infinite. Thus, given the estimated subgroup membership, we may write $\hat{\alpha}(t) = (\hat{\alpha}_1(t), \dots, \hat{\alpha}_K(t))^T$ for any given $t \in \mathbb{T}$, and the following theorem holds.

Theorem 4 Under the same conditions in Theorem 3. If $J_n/m_{(n)}^{1/(2r+1)} \rightarrow \infty$, we have

$$\text{Var}(\hat{\boldsymbol{\alpha}}(t))^{-1/2}(\hat{\boldsymbol{\alpha}}(t) - \boldsymbol{\alpha}(t)) \xrightarrow{d} N(\mathbf{0}, \mathbf{I}_K),$$

where \mathbf{I}_K is a K -dimensional identity matrix and

$$\text{Var}(\hat{\boldsymbol{\alpha}}(t)) = \mathbb{B}(t) (\mathbf{X}^T \mathbf{V}^{-1} \mathbf{X})^{-1} (\mathbf{X}^T \mathbf{V}^{-1} \boldsymbol{\Sigma} \mathbf{V}^{-1} \mathbf{X}) (\mathbf{X}^T \mathbf{V}^{-1} \mathbf{X})^{-1} \mathbb{B}(t)^T,$$

with $\mathbf{B}(t) = (B_1(t), \dots, B_d(t))^T$ and $\mathbb{B}(t) = \mathbf{I}_K \otimes \mathbf{B}(t)^T$. In particular,

$$\text{Var}(\hat{\alpha}_k(t))^{-1/2}(\hat{\alpha}_k(t) - \alpha_k(t)) \xrightarrow{d} N(0, 1)$$

for $k = 1, \dots, K$, where $\text{Var}(\hat{\alpha}_k(t)) = \mathbf{e}_k^T \text{Var}(\hat{\boldsymbol{\alpha}}(t)) \mathbf{e}_k$, and \mathbf{e}_k is the K -dimensional vector with the k th element taken to be 1 and 0 elsewhere.

We can use the asymptotic distribution established in Theorem 4 to construct pointwise confidence intervals of the functional curve for each subgroup.

5 Simulation studies

In this section, we investigate the performance of our proposed approach by conducting simulation studies. Balanced and unbalanced data are both considered.

Two different criteria are used to select the optimal tuning parameter. One is the modified Bayes Information Criterion (BIC) for high-dimensional data settings by minimizing

$$\text{BIC}(\lambda) = \log \left[\sum_{i=1}^n (\mathbf{Y}_i - \mathbf{X}_i \hat{\boldsymbol{\gamma}}_i(\lambda))^T \mathbf{R}_i^{-1} (\mathbf{Y}_i - \mathbf{X}_i \hat{\boldsymbol{\gamma}}_i(\lambda)) / N \right] + C_n \frac{\log N}{N} (\hat{K}(\lambda)d), \quad (5.1)$$

where C_n is a positive number which can depend on n and $N = \sum_{i=1}^n m_i$. Following [Ma and Huang \(2017\)](#), we let $C_n = c \log(\log(nd))$, where c is a positive constant, and we choose $c = 0.6$ in the simulation studies. The other criterion is the Calinski-Harabasz index ([Caliński and Harabasz, 1974](#)) by maximizing

$$\text{CH}(\lambda) = \frac{B_{\hat{K}(\lambda)} / (\hat{K}(\lambda) - 1)}{W_{\hat{K}(\lambda)} / (n - \hat{K}(\lambda))}, \quad (5.2)$$

where $B_{\hat{K}(\lambda)}$ and $W_{\hat{K}(\lambda)}$ are the between and within group sum of square errors of the estimated subgroups given a λ value. We apply this index to the initial value $\boldsymbol{\gamma}_i^0$'s presented in Subsection

A.1.1. Note that $\text{CH}(\lambda)$ is not defined for $\hat{K}(\lambda) = 1$. Based on these criteria, we can select the optimal λ and obtain the corresponding group membership. Here we use fixed values for ϑ and τ in ADMM algorithm: $\vartheta = 1$ and $\tau = 3$.

To evaluate the accuracy of the clustering results, we provide three measures: Rand Index (RI) (Rand, 1971), Normalized Mutual Information (NMI) (Vinh et al., 2010) and accuracy percentage (%). We define the accuracy percentage (%) by the proportion of subjects that are correctly identified. These three values are between 0 and 1, with higher values indicating better performance.

5.1 Two Subgroups Example

We simulate data from the heterogeneous model with two subgroups

$$Y_{ij} = \beta_i(t_{ij}) + \varepsilon_{ij}, \quad i = 1, \dots, n, \quad j = 1, \dots, m_i,$$

where $\beta_i(t) = \alpha_1(t)$ if $i \in \mathcal{G}_1$ and $\beta_i(t) = \alpha_2(t)$ if $i \in \mathcal{G}_2$.

We first consider balanced data. In this situation, we have $m_i = T$ for all i 's. The time points t_{ij} 's are chosen equally spaced on $[0, 1.2]$. The error term $\varepsilon_i = (\varepsilon_{i1}, \dots, \varepsilon_{iT})^T$ is generated from $N(\mathbf{0}, \Sigma_E)$, in which Σ_E has AR(1) covariance structure with $\rho = 0.3$ and $\sigma = 0.5$. We consider 4 setups of $\{n, T\}$: $\{n = 100, T = 20\}$, $\{n = 100, T = 50\}$, $\{n = 150, T = 20\}$ and $\{n = 150, T = 50\}$. Moreover, to choose $\{\alpha_1(t), \alpha_2(t)\}$, we also consider three different cases by increasing the distance between the two functions from close to middle, then to far, which are shown below:

$$\text{Close} \begin{cases} \alpha_1(t) = -0.5t^2 + 1.25t, \\ \alpha_2(t) = -t^2 + 2.5t, \end{cases} \quad \text{Middle} \begin{cases} \alpha_1(t) = -0.5t^2 + 1.25t, \\ \alpha_2(t) = -1.3t^2 + 3.25t, \end{cases} \quad \text{Far} \begin{cases} \alpha_1(t) = -0.5t^2 + 1.25t, \\ \alpha_2(t) = -2.5t^2 + 6.25t. \end{cases}$$

Figure 2 shows the true functions (black line) and simulated trajectories (blue line and red line) of the three distance cases, respectively, based on one sample with $n = 100, T = 20$ for balanced data. We can see that there are a lot of overlaps in close and middle case, especially in close case, it looks more like one group.

The unbalanced data is based on the balanced data setting. However, we randomly allow 50% of the subjects to miss either 30% or 40% or 50% of time points. Next, we conduct simulations to illustrate the performance of our proposed method. Quadratic splines with one interior knot are used to approximate the nonparametric components. 100 replications are taken here.

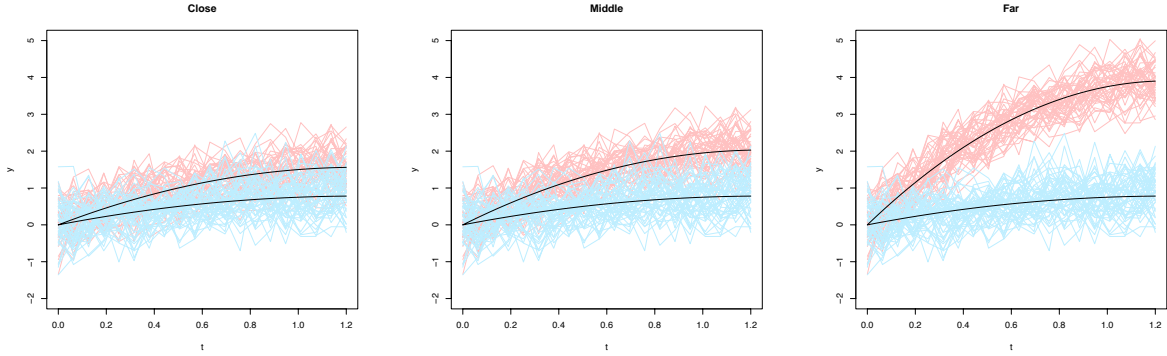


Fig. 2: The black lines represent the true functions, while the red and blue lines represent the simulated trajectories of the corresponding subgroups under one replication when $n = 100$, $T = 20$ for balanced data in Two Subgroups Example. The distance between the true functions increases from close, to middle, to far.

Table 1 not only reports the summary measurements of the estimated number of subgroups \hat{K} (sample mean, median, per, where per is the percentage of \hat{K} equaling to the true number of subgroups), but also the summary measurements of the clustering accuracy (average values of RI, NMI, %) by using different model selection criteria (BIC, CH) under different setups of $\{n, T\}$ when the distance between functions increases (Close, Middle, Far). Balanced and unbalanced data are both included. Note that when calculating RI, NMI and %, we only consider the replications with \hat{K} equaling to the true number of subgroup ($\hat{K} = 2$).

From Table 1, we can see that both BIC and CH criteria perform well and give the similar results for most of the cases. When T increases, the summary measurements of \hat{K} (mean, median, per) and accuracy measurements (RI, NMI, %) both increase. In details, the mean of \hat{K} gets close to 2 and median \hat{K} becomes to 2, where 2 is the true number of subgroups, while the accuracy measurements (RI, NMI, %) are close to 1 or even become to 1 for both balanced and unbalanced data, which indicates good clustering results. What's more, with the distance between the true functions getting larger, it is much easier to correctly identify the subgroups. Accordingly, we observe that the mean and median of \hat{K} become to 2, while the RI, NMI and % become to 1 when the distance is sufficiently large (Far case). On the contrary, in close case, since the trajectories of the two subgroups in Figure 2 show a lot of overlaps, it is more difficult to identify the subgroups, which results in the low percentage (per) of correctly selecting the number of subgroups when $T = 20$. Under this case, if we can cluster the subjects into two subgroups, BIC criterion presents higher

accuracy performance in group membership. However, if T increases to 50, all the measurements become much better and it is more likely to correctly identify the subgroups. Compared with unbalanced data, balanced data shows slightly better results.

Furthermore, to study the estimation accuracy, we calculate the square root of the mean squared error (RMSE) of the estimated functions respectively only when \hat{K} equals the true number of subgroups ($\hat{K} = 2$). In the k th subgroup, we use the formula below to find the corresponding RMSE of the estimated function $\hat{\alpha}_k(t)$ (RMSE $_k$):

$$\text{RMSE}_k = \sqrt{\frac{1}{H} \sum_{h=1}^H [\hat{\alpha}_k(t_h) - \alpha_k(t_h)]^2} \approx \sqrt{\frac{1}{H} \sum_{h=1}^H [\mathbf{B}_k^T(t_h) \hat{\gamma}_{(k)} - \alpha_k(t_h)]^2}, \quad k = 1, 2,$$

where $\mathbf{B}_k(t)$ is the B-spline basis vector of this subgroup, $\hat{\gamma}_{(k)}$ is the corresponding estimated B-spline coefficient after refitting model (3.2) and $\{t_1, \dots, t_H\}$ is a time sequence chosen on $[0, 1.2]$. For oracle (Oracle) method, we use the true group membership to calculate RMSE. As shown in Table 2, the RMSE values under different model selection criteria (BIC, CH) and $\{n, T\}$ setups are comparable to those of the oracle ones for almost all cases.

Lastly, the estimated nonparametric curves $\hat{\alpha}_k(t)$ (blue, red lines) and true curves $\alpha_k(t)$ (black line) of the two subgroups for balanced data among the 100 replications are plotted in Figure 3. Notice that we only plot the replications when the estimated number of subgroups equals the true number of subgroups ($\hat{K} = 2$). On each row, from left to right, it represents the close, middle, and far cases with same setting of $\{n, T\}$ respectively. Then either n or T is increased compared to the first row. Given each column, it is obvious that the bands consisting by red or blue lines becomes narrower as T or n increases. Besides, no matter for which setups of $\{n, T\}$, the estimated curves are very close to the true ones for all distance cases. In a word, simulation results confirm that our proposed approach performs very well on clustering the heterogeneous trajectories.

5.2 Three Subgroups Example

We simulate data from the heterogeneous model with three subgroups

$$Y_{ij} = \beta_i(t_{ij}) + \varepsilon_{ij}, \quad i = 1, \dots, n, \quad j = 1, \dots, m_i,$$

where $\beta_i(t) = \alpha_1(t)$ if $i \in \mathcal{G}_1$, $\beta_i(t) = \alpha_2(t)$ if $i \in \mathcal{G}_2$ and $\beta_i(t) = \alpha_3(t)$ if $i \in \mathcal{G}_3$. We generate data in the same way as that in Two Subgroups Example. The three functions for close, middle and far

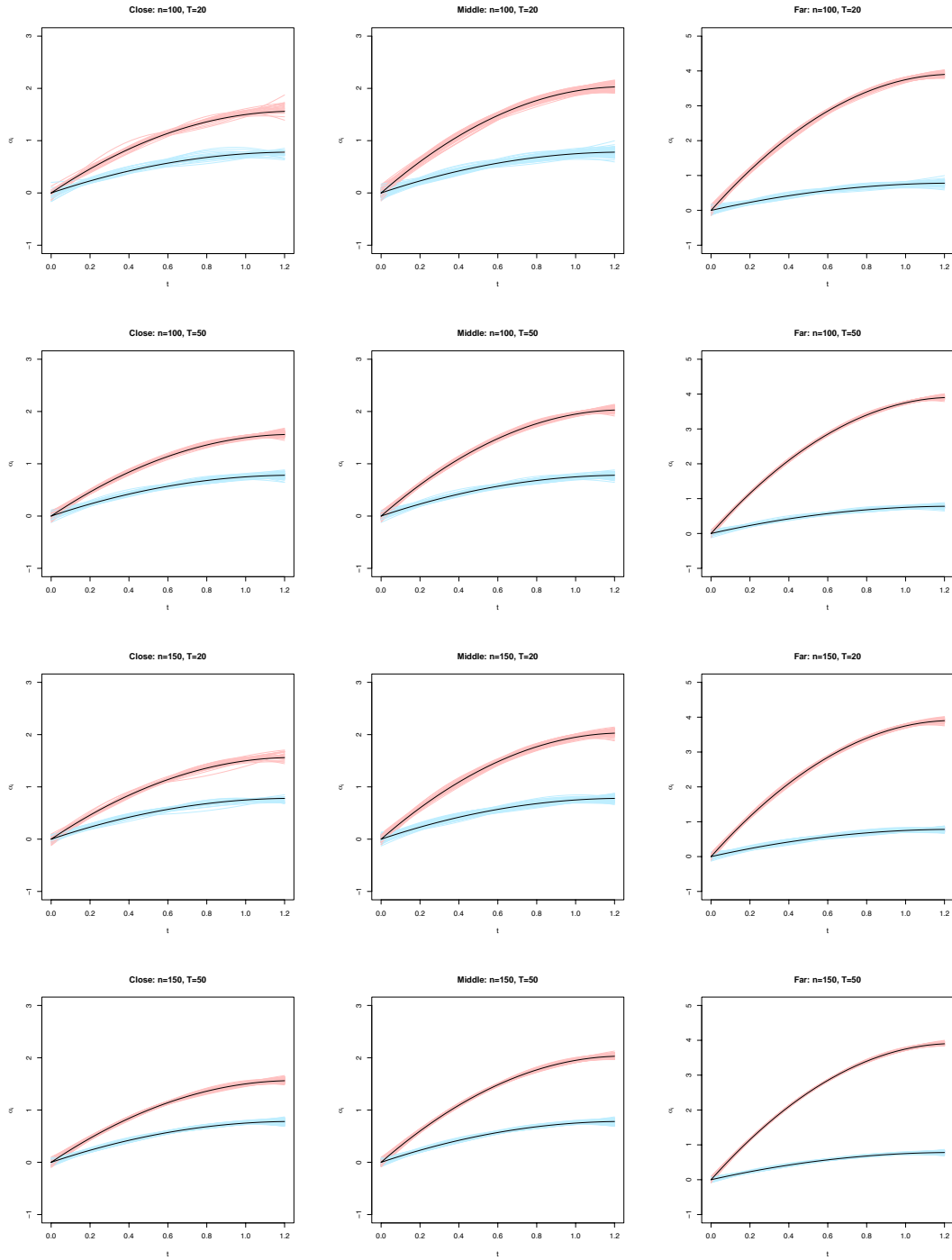


Fig. 3: The black lines represent the true functions, while the red and blue lines are the corresponding fitted curves for the estimated subgroups by using BIC criterion when $\hat{K} = 2$ among the 100 replications for balanced data in Two Subgroups Example. On each row, from left to right, it corresponds to close, middle, and far cases with the same setting of $\{n, T\}$.

			Balanced						Unbalanced					
Functions	setting	criterion	mean	median	per	RI	NMI	%	mean	median	per	RI	NMI	%
Close	n=100, T=20	BIC	1.34	1.00	0.20	0.9089	0.7459	0.9515	1.43	1.00	0.08	0.9015	0.7289	0.9475
		CH	1.55	1.00	0.35	0.8730	0.6818	0.9223	1.73	1.50	0.28	0.7652	0.4861	0.8304
	n=100, T=50	BIC	1.98	2.00	0.98	0.9953	0.9836	0.9977	1.97	2.00	0.97	0.9855	0.9510	0.9927
		CH	1.98	2.00	0.98	0.9953	0.9834	0.9977	1.97	2.00	0.97	0.9855	0.9510	0.9927
	n=150, T=20	BIC	1.45	1.00	0.23	0.9271	0.7820	0.9620	1.50	1.00	0.08	0.8868	0.6855	0.9400
		CH	1.57	1.00	0.31	0.8746	0.6876	0.9178	1.74	1.00	0.26	0.6451	0.2757	0.7015
	n=150, T=50	BIC	2.00	2.00	1.00	0.9923	0.9719	0.9961	2.00	2.00	1.00	0.9855	0.9484	0.9927
		CH	2.00	2.00	1.00	0.9922	0.9717	0.9961	1.98	2.00	0.98	0.9852	0.9472	0.9925
			Balanced						Unbalanced					
Functions	setting	criterion	mean	median	per	RI	NMI	%	mean	median	per	RI	NMI	%
Middle	n=100, T=20	BIC	2.00	2.00	1.00	0.9960	0.9859	0.9980	2.00	2.00	1.00	0.9903	0.9664	0.9951
		CH	2.00	2.00	1.00	0.9952	0.9830	0.9976	2.00	2.00	1.00	0.9901	0.9655	0.9950
	n=100, T=50	BIC	2.00	2.00	1.00	0.9998	0.9993	0.9999	2.00	2.00	1.00	0.9996	0.9985	0.9998
		CH	2.00	2.00	1.00	0.9998	0.9993	0.9999	2.00	2.00	1.00	0.9996	0.9985	0.9998
	n=150, T=20	BIC	2.00	2.00	1.00	0.9967	0.9870	0.9983	2.01	2.00	0.99	0.9874	0.9535	0.9937
		CH	2.00	2.00	1.00	0.9967	0.9870	0.9983	2.00	2.00	1.00	0.9865	0.9503	0.9932
	n=150, T=50	BIC	2.00	2.00	1.00	1.0000	1.0000	1.0000	2.00	2.00	1.00	0.9999	0.9995	0.9999
		CH	2.00	2.00	1.00	0.9999	0.9995	0.9999	2.00	2.00	1.00	0.9997	0.9990	0.9999
			Balanced						Unbalanced					
Functions	setting	criterion	mean	median	per	RI	NMI	%	mean	median	per	RI	NMI	%
Far	n=100, T=20	BIC	2.00	2.00	1.00	1.0000	1.0000	1.0000	2.00	2.00	1.00	1.0000	1.0000	1.0000
		CH	2.00	2.00	1.00	1.0000	1.0000	1.0000	2.00	2.00	1.00	1.0000	1.0000	1.0000
	n=100, T=50	BIC	2.00	2.00	1.00	1.0000	1.0000	1.0000	2.00	2.00	1.00	1.0000	1.0000	1.0000
		CH	2.00	2.00	1.00	1.0000	1.0000	1.0000	2.00	2.00	1.00	1.0000	1.0000	1.0000
	n=150, T=20	BIC	2.00	2.00	1.00	1.0000	1.0000	1.0000	2.00	2.00	1.00	1.0000	1.0000	1.0000
		CH	2.00	2.00	1.00	1.0000	1.0000	1.0000	2.00	2.00	1.00	1.0000	1.0000	1.0000
	n=150, T=50	BIC	2.00	2.00	1.00	1.0000	1.0000	1.0000	2.00	2.00	1.00	1.0000	1.0000	1.0000
		CH	2.00	2.00	1.00	1.0000	1.0000	1.0000	2.00	2.00	1.00	1.0000	1.0000	1.0000

Table 1: The sample mean and median of \hat{K} , the percentage (per) of \hat{K} equaling to the true number of subgroups, the Rand Index (RI), Normalized mutual information (NMI), and accuracy percentage (%) equaling the proportion of subjects that are identified correctly under BIC and CH criteria based on 100 realizations in Two Subgroups Example. Balanced and unbalanced data are both included under different $\{n, T\}$ setups and function distances.

cases are chosen as:

$$\begin{aligned}
\text{Close} & \begin{cases} \alpha_1(t) = -0.6t^2 + 1.5t, \\ \alpha_2(t) = -1.3t^2 + 3.25t + 0.2, \\ \alpha_3(t) = -2.2t^2 + 5.5t + 0.1, \end{cases} & \text{Middle} & \begin{cases} \alpha_1(t) = -0.4t^2 + t, \\ \alpha_2(t) = -1.3t^2 + 3.25t + 0.2, \\ \alpha_3(t) = -2.4t^2 + 6t + 0.1, \end{cases} \\
\text{Far} & \begin{cases} \alpha_1(t) = -0.3t^2 + 0.75t, \\ \alpha_2(t) = -4t^2 + 10t + 0.2, \\ \alpha_3(t) = -8.5t^2 + 21.25t + 0.3. \end{cases}
\end{aligned}$$

Figure 4 displays the true functions and corresponding trajectories of the three subgroups under one sample with $n = 100$, $T = 20$ for balanced data. From left to right, the distance between true functions gets larger. We next conduct simulations to do subgroup analysis by using our method. Table 3, based on 100 realizations, presents the mean, median, per of \hat{K} and the average values of RI, NMI, % for all setups under BIC and CH criteria, respectively. In this table, we observe that the performance for balanced data is better than the corresponding unbalanced data. BIC and CH criteria are consistent due to similar results. When T or the distance between true functions increases, the values of RI, NMI, and % become larger. Moreover, to demonstrate the estimation accuracy, Table 4 lists the average values of RMSE for the estimated functions $\hat{\alpha}_k(t)$ ($k = 1, 2, 3$) when \hat{K} equals 3, while Figure 5 shows the estimated nonparametric curves (grey, red, blue lines)

	Close				Middle				Far			
	Balanced		Unbalanced		Balanced		Unbalanced		Balanced		Unbalanced	
$n=100, T=20$	$\hat{\alpha}_1(t)$	$\hat{\alpha}_2(t)$	$\hat{\alpha}_1(t)$	$\hat{\alpha}_2(t)$	$\hat{\alpha}_1(t)$	$\hat{\alpha}_2(t)$	$\hat{\alpha}_1(t)$	$\hat{\alpha}_2(t)$	$\hat{\alpha}_1(t)$	$\hat{\alpha}_2(t)$	$\hat{\alpha}_1(t)$	$\hat{\alpha}_2(t)$
Oracle	0.0363	0.0369	0.0382	0.0399	0.0363	0.0369	0.0382	0.0401	0.0363	0.0369	0.0382	0.0413
BIC	0.0512	0.0467	0.0570	0.0448	0.0365	0.0377	0.0391	0.0408	0.0363	0.0369	0.0382	0.0413
CH	0.0626	0.0610	0.1049	0.1144	0.0364	0.0375	0.0392	0.0407	0.0363	0.0369	0.0382	0.0413
$n=100, T=50$	$\hat{\alpha}_1(t)$	$\hat{\alpha}_2(t)$	$\hat{\alpha}_1(t)$	$\hat{\alpha}_2(t)$	$\hat{\alpha}_1(t)$	$\hat{\alpha}_2(t)$	$\hat{\alpha}_1(t)$	$\hat{\alpha}_2(t)$	$\hat{\alpha}_1(t)$	$\hat{\alpha}_2(t)$	$\hat{\alpha}_1(t)$	$\hat{\alpha}_2(t)$
Oracle	0.0247	0.0235	0.0259	0.0241	0.0247	0.0235	0.0259	0.0241	0.0247	0.0235	0.0259	0.0242
BIC	0.0253	0.0236	0.0274	0.0250	0.0248	0.0234	0.0260	0.0240	0.0247	0.0235	0.0259	0.0242
CH	0.0253	0.0237	0.0273	0.0251	0.0248	0.0234	0.0260	0.0240	0.0247	0.0235	0.0259	0.0242
$n=150, T=20$	$\hat{\alpha}_1(t)$	$\hat{\alpha}_2(t)$	$\hat{\alpha}_1(t)$	$\hat{\alpha}_2(t)$	$\hat{\alpha}_1(t)$	$\hat{\alpha}_2(t)$	$\hat{\alpha}_1(t)$	$\hat{\alpha}_2(t)$	$\hat{\alpha}_1(t)$	$\hat{\alpha}_2(t)$	$\hat{\alpha}_1(t)$	$\hat{\alpha}_2(t)$
Oracle	0.0314	0.0281	0.0334	0.0307	0.0314	0.0281	0.0334	0.0310	0.0314	0.0281	0.0334	0.0330
BIC	0.0387	0.0403	0.0447	0.0433	0.0317	0.0282	0.0341	0.0310	0.0314	0.0281	0.0334	0.0330
CH	0.0602	0.0606	0.1856	0.1788	0.0317	0.0281	0.0344	0.0311	0.0314	0.0281	0.0334	0.0330
$n=150, T=50$	$\hat{\alpha}_1(t)$	$\hat{\alpha}_2(t)$	$\hat{\alpha}_1(t)$	$\hat{\alpha}_2(t)$	$\hat{\alpha}_1(t)$	$\hat{\alpha}_2(t)$	$\hat{\alpha}_1(t)$	$\hat{\alpha}_2(t)$	$\hat{\alpha}_1(t)$	$\hat{\alpha}_2(t)$	$\hat{\alpha}_1(t)$	$\hat{\alpha}_2(t)$
Oracle	0.0199	0.0212	0.0212	0.0221	0.0199	0.0212	0.0212	0.0221	0.0199	0.0212	0.0212	0.0225
BIC	0.0204	0.0217	0.0220	0.0228	0.0199	0.0212	0.0212	0.0221	0.0199	0.0212	0.0212	0.0225
CH	0.0204	0.0217	0.0218	0.0228	0.0199	0.0212	0.0212	0.0221	0.0199	0.0212	0.0212	0.0225

Table 2: The mean of square root of the MSE (RMSE) for the estimated functions $\hat{\alpha}_1(t), \hat{\alpha}_2(t)$ under BIC, CH and Oracle methods in Two Subgroups Example.

and true curves (black lines). From Table 4, it can be seen that the RMSE of $\hat{\alpha}_k(t)$'s are close to those of the oracle estimators. In Figure 5, we also observe that the estimated curves are very close to the true curves. And the bands formed by the corresponding estimated curves become narrower as n or T increases.

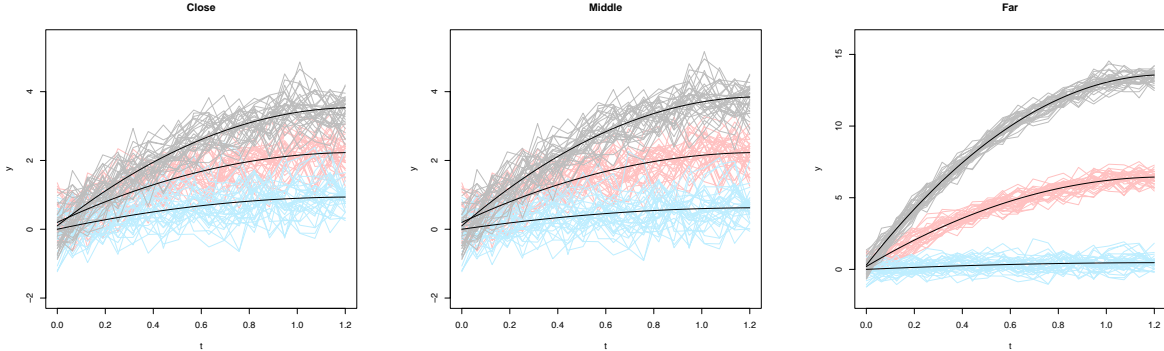


Fig. 4: The black lines represent the true functions, while the grey, red and blue lines represent the simulated trajectories of the corresponding subgroups under one replication when $n = 100, T = 20$ for balanced data. The distance between the true functions increases from close, to middle, to far.

6 Real data application

In this section, we apply our method to Alzheimer's disease (AD) data, which can be obtained from the Alzheimer's Disease Neuroimaging Initiative (ADNI) database (adni.loni.usc.edu). The ADNI was launched in 2003 as a public-private partnership, led by Principal Investigator Michael W. Weiner, MD. The primary goal of ADNI has been to test whether serial magnetic resonance imaging (MRI), positron emission tomography (PET), other biological markers, and clinical and neuropsych-

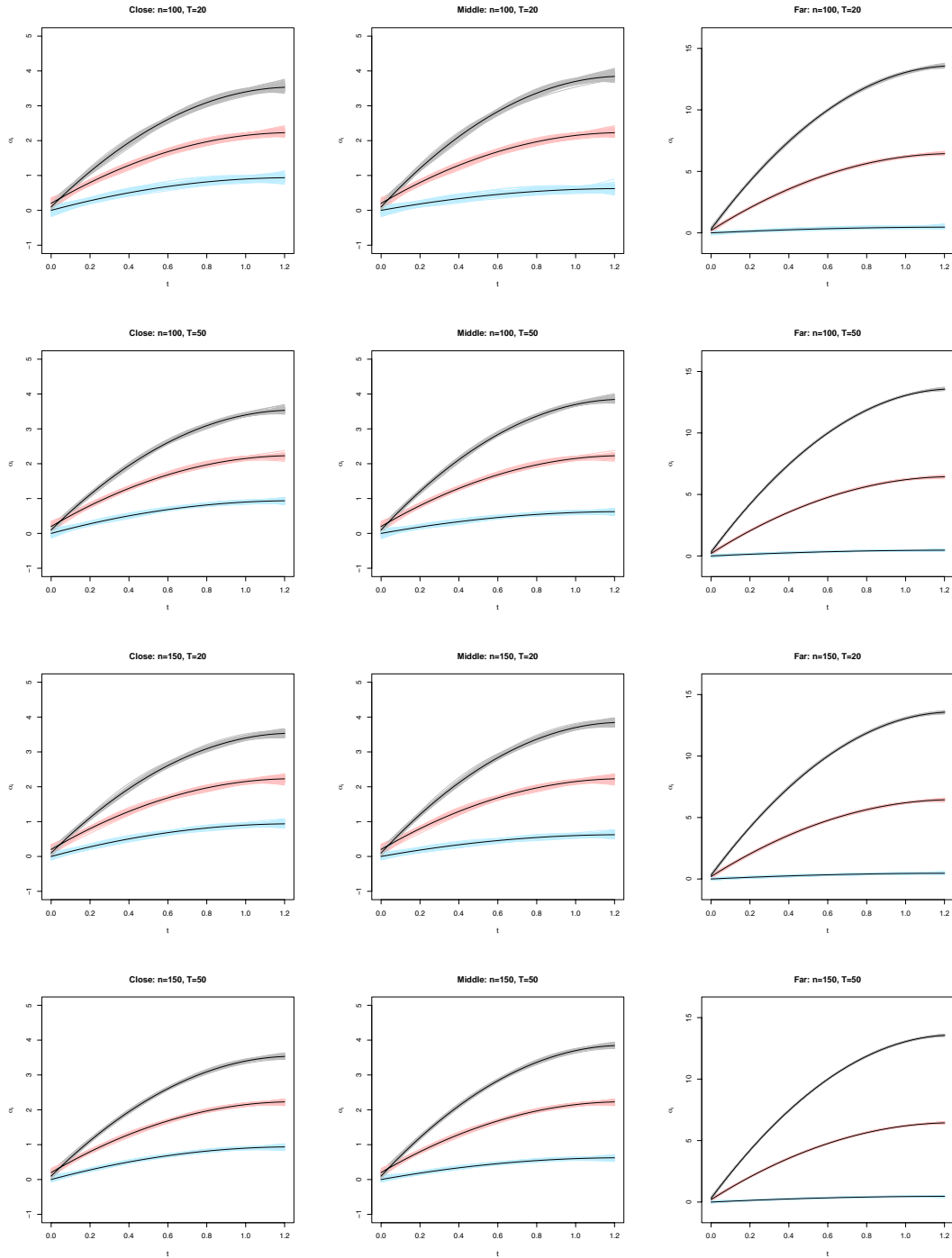


Fig. 5: The black lines represent the true functions, while the grey, red and blue lines are the corresponding fitted curves for the estimated subgroups by using BIC criterion when $\hat{K} = 3$ among the 100 replications for balanced data in Three Subgroups Example. On each row, from left to right, it corresponds to close, middle, and far cases with the same setting of $\{n, T\}$.

Functions	setting	criterion	Balanced						Unbalanced					
			mean	median	per	RI	NMI	%	mean	median	per	RI	NMI	%
Close	n=100, T=20	BIC	3.00	3.00	1.00	0.9962	0.9882	0.9971	3.00	3.00	1.00	0.9870	0.9603	0.9899
		CH	2.79	3.00	0.79	0.9965	0.9891	0.9973	2.52	3.00	0.52	0.9887	0.9665	0.9915
	n=100, T=50	BIC	2.98	3.00	0.98	1.0000	1.0000	1.0000	2.98	3.00	0.98	0.9998	0.9993	0.9998
		CH	2.98	3.00	0.98	1.0000	1.0000	1.0000	2.96	3.00	0.98	0.9996	0.9988	0.9997
	n=150, T=20	BIC	3.00	3.00	1.00	0.9982	0.9939	0.9987	3.01	3.00	0.99	0.9910	0.9709	0.9931
		CH	2.91	3.00	0.91	0.9982	0.9940	0.9987	2.69	3.00	0.69	0.9903	0.9691	0.9928
	n=150, T=50	BIC	3.00	3.00	1.00	1.0000	1.0000	1.0000	3.00	3.00	1.00	0.9999	0.9997	0.9999
		CH	3.00	3.00	1.00	1.0000	1.0000	1.0000	3.00	3.00	1.00	0.9999	0.9997	0.9999
Functions	setting	criterion	Balanced						Unbalanced					
			mean	median	per	RI	NMI	%	mean	median	per	RI	NMI	%
Middle	n=100, T=20	BIC	3.00	3.00	1.00	0.9996	0.9987	0.9997	3.00	3.00	1.00	0.9965	0.9889	0.9973
		CH	3.00	3.00	1.00	0.9995	0.9983	0.9996	2.98	3.00	0.98	0.9962	0.9880	0.9970
	n=100, T=50	BIC	3.00	3.00	1.00	1.0000	1.0000	1.0000	3.00	3.00	1.00	1.0000	1.0000	1.0000
		CH	3.00	3.00	1.00	1.0000	1.0000	1.0000	3.00	3.00	1.00	1.0000	1.0000	1.0000
	n=150, T=20	BIC	3.00	3.00	1.00	0.9998	0.9994	0.9999	3.00	3.00	1.00	0.9978	0.9925	0.9983
		CH	3.00	3.00	1.00	0.9999	0.9997	0.9999	3.00	3.00	1.00	0.9978	0.9929	0.9984
	n=150, T=50	BIC	3.00	3.00	1.00	1.0000	1.0000	1.0000	3.00	3.00	1.00	1.0000	1.0000	1.0000
		CH	3.00	3.00	1.00	1.0000	1.0000	1.0000	3.00	3.00	1.00	1.0000	1.0000	1.0000
Functions	setting	criterion	Balanced						Unbalanced					
			mean	median	per	RI	NMI	%	mean	median	per	RI	NMI	%
Far	n=100, T=20	BIC	3.00	3.00	1.00	1.0000	1.0000	1.0000	3.00	3.00	1.00	1.0000	1.0000	1.0000
		CH	3.00	3.00	1.00	1.0000	1.0000	1.0000	3.00	3.00	1.00	1.0000	1.0000	1.0000
	n=100, T=50	BIC	3.00	3.00	1.00	1.0000	1.0000	1.0000	3.00	3.00	1.00	1.0000	1.0000	1.0000
		CH	3.00	3.00	1.00	1.0000	1.0000	1.0000	3.00	3.00	1.00	1.0000	1.0000	1.0000
	n=150, T=20	BIC	3.00	3.00	1.00	1.0000	1.0000	1.0000	3.00	3.00	1.00	1.0000	1.0000	1.0000
		CH	3.00	3.00	1.00	1.0000	1.0000	1.0000	3.00	3.00	1.00	1.0000	1.0000	1.0000
	n=150, T=50	BIC	3.00	3.00	1.00	1.0000	1.0000	1.0000	3.00	3.00	1.00	1.0000	1.0000	1.0000
		CH	3.00	3.00	1.00	1.0000	1.0000	1.0000	3.00	3.00	1.00	1.0000	1.0000	1.0000

Table 3: The sample mean and median of \hat{K} , the percentage (per) of \hat{K} equaling to the true number of subgroups, the Rand Index (RI), Normalized mutual information (NMI), and accuracy percentage (%) equaling the proportion of subjects that are identified correctly under BIC and CH criteria based on 100 realizations in Three Subgroups Example. Balanced and unbalanced data are both considered under different $\{n, T\}$ setups and function distances.

chological assessment can be combined to measure the progression of mild cognitive impairment (MCI) and early Alzheimer’s disease (AD). For up-to-date information, see www.adni-info.org.

We consider the longitudinal data for ADASCOG13 (Alzheimer’s Disease Assessment Scale-Cognitive Subscale) for each patient from ADNI1, ADNIGO and ADNI2 at 13 different time points (0, 6, 12, 18, 24, 36, 48, 60, 72, 84, 96, 108, 120 months). ADASCOG13 is widely used as test of cognitive functions, consisting of 13 tests with the range from 0 to 85 to assess the severity of the dementia. Higher values indicate more severe of the dementia due to more cognitive errors. We first removed incomplete observations. In order to implement our cluster procedure, patients with less than 4 visits were removed. Therefore, in total, we have 1251 patients.

Next, we used ADASCOG13 as the response to fit the heterogeneous model (2.3). All of the ADASCOG13 values were standardized before applying our method. Quadratic splines with one knot are taken to approximate the nonparametric part. When utilizing BIC selection criterion given in (5.1), we let $C_n = 1.5 \log(\log(nd))$. The clustering results indicate the presence of two subgroups, which was shown in Figure 6. The 1251 patients were identified as one big subgroup

	Close						Middle						Far					
	Balanced			Unbalanced			Balanced			Unbalanced			Balanced			Unbalanced		
n=100, T=20	$\hat{\alpha}_1(t)$	$\hat{\alpha}_2(t)$	$\hat{\alpha}_3(t)$	$\hat{\alpha}_1(t)$	$\hat{\alpha}_2(t)$	$\hat{\alpha}_3(t)$	$\hat{\alpha}_1(t)$	$\hat{\alpha}_2(t)$	$\hat{\alpha}_3(t)$	$\hat{\alpha}_1(t)$	$\hat{\alpha}_2(t)$	$\hat{\alpha}_3(t)$	$\hat{\alpha}_1(t)$	$\hat{\alpha}_2(t)$	$\hat{\alpha}_3(t)$	$\hat{\alpha}_1(t)$	$\hat{\alpha}_2(t)$	$\hat{\alpha}_3(t)$
Oracle	0.0472	0.0430	0.0465	0.0503	0.0457	0.0529	0.0472	0.0430	0.0465	0.0503	0.0457	0.0534	0.0472	0.0430	0.0465	0.0504	0.0495	0.0733
BIC	0.0466	0.0447	0.0470	0.0507	0.0481	0.0528	0.0469	0.0432	0.0467	0.0500	0.0465	0.0528	0.0472	0.0430	0.0465	0.0504	0.0495	0.0733
CH	0.0466	0.0425	0.0474	0.0538	0.0436	0.0515	0.0469	0.0433	0.0467	0.0499	0.0459	0.0529	0.0472	0.0430	0.0465	0.0504	0.0495	0.0733
n=100, T=50	$\hat{\alpha}_1(t)$	$\hat{\alpha}_2(t)$	$\hat{\alpha}_3(t)$	$\hat{\alpha}_1(t)$	$\hat{\alpha}_2(t)$	$\hat{\alpha}_3(t)$	$\hat{\alpha}_1(t)$	$\hat{\alpha}_2(t)$	$\hat{\alpha}_3(t)$	$\hat{\alpha}_1(t)$	$\hat{\alpha}_2(t)$	$\hat{\alpha}_3(t)$	$\hat{\alpha}_1(t)$	$\hat{\alpha}_2(t)$	$\hat{\alpha}_3(t)$	$\hat{\alpha}_1(t)$	$\hat{\alpha}_2(t)$	$\hat{\alpha}_3(t)$
Oracle	0.0300	0.0295	0.0316	0.0312	0.0315	0.0332	0.0300	0.0295	0.0316	0.0312	0.0315	0.0334	0.0300	0.0295	0.0316	0.0312	0.0317	0.0381
BIC	0.0299	0.0297	0.0317	0.0310	0.0318	0.0334	0.0300	0.0295	0.0316	0.0312	0.0315	0.0334	0.0300	0.0295	0.0316	0.0312	0.0317	0.0381
CH	0.0299	0.0297	0.0317	0.0310	0.0318	0.0333	0.0300	0.0295	0.0316	0.0312	0.0315	0.0334	0.0300	0.0295	0.0316	0.0312	0.0317	0.0381
n=150, T=20	$\hat{\alpha}_1(t)$	$\hat{\alpha}_2(t)$	$\hat{\alpha}_3(t)$	$\hat{\alpha}_1(t)$	$\hat{\alpha}_2(t)$	$\hat{\alpha}_3(t)$	$\hat{\alpha}_1(t)$	$\hat{\alpha}_2(t)$	$\hat{\alpha}_3(t)$	$\hat{\alpha}_1(t)$	$\hat{\alpha}_2(t)$	$\hat{\alpha}_3(t)$	$\hat{\alpha}_1(t)$	$\hat{\alpha}_2(t)$	$\hat{\alpha}_3(t)$	$\hat{\alpha}_1(t)$	$\hat{\alpha}_2(t)$	$\hat{\alpha}_3(t)$
Oracle	0.0353	0.0373	0.0355	0.0383	0.0400	0.0390	0.0353	0.0373	0.0355	0.0381	0.0400	0.0392	0.0353	0.0373	0.0355	0.0381	0.0452	0.0557
BIC	0.0353	0.0376	0.0357	0.0395	0.0414	0.0396	0.0353	0.0374	0.0356	0.0383	0.0403	0.0393	0.0353	0.0373	0.0355	0.0381	0.0452	0.0557
CH	0.0345	0.0360	0.0356	0.0381	0.0409	0.0402	0.0353	0.0374	0.0355	0.0383	0.0404	0.0393	0.0353	0.0373	0.0355	0.0381	0.0452	0.0557
n=150, T=50	$\hat{\alpha}_1(t)$	$\hat{\alpha}_2(t)$	$\hat{\alpha}_3(t)$	$\hat{\alpha}_1(t)$	$\hat{\alpha}_2(t)$	$\hat{\alpha}_3(t)$	$\hat{\alpha}_1(t)$	$\hat{\alpha}_2(t)$	$\hat{\alpha}_3(t)$	$\hat{\alpha}_1(t)$	$\hat{\alpha}_2(t)$	$\hat{\alpha}_3(t)$	$\hat{\alpha}_1(t)$	$\hat{\alpha}_2(t)$	$\hat{\alpha}_3(t)$	$\hat{\alpha}_1(t)$	$\hat{\alpha}_2(t)$	$\hat{\alpha}_3(t)$
Oracle	0.0226	0.0255	0.0250	0.0249	0.0274	0.0270	0.0226	0.0255	0.0250	0.0249	0.0274	0.0271	0.0226	0.0255	0.0250	0.0249	0.0287	0.0318
BIC	0.0226	0.0255	0.0250	0.0249	0.0274	0.0270	0.0226	0.0255	0.0250	0.0249	0.0274	0.0271	0.0226	0.0255	0.0250	0.0249	0.0287	0.0318
CH	0.0226	0.0255	0.0250	0.0249	0.0274	0.0270	0.0226	0.0255	0.0250	0.0249	0.0274	0.0271	0.0226	0.0255	0.0250	0.0249	0.0287	0.0318

Table 4: The mean of square root of the MSE (RMSE) for the estimated functions $\hat{\alpha}_1(t), \hat{\alpha}_2(t), \hat{\alpha}_3(t)$ under BIC, CH and Oracle methods in Three Subgroups Example.

with 950 patients and one small subgroup with 301 patients. The big subgroup could be viewed as a ‘non-progression group’ as depicted in red since the patients’ cognition did not get worse, while the small one could be viewed as ‘progression group’ as depicted in blue as the disease among these patients get severe over time. Therefore, the progression group was potentially of interest to be recruited in clinical trials when testing whether the drug could slow down the cognitive decline.

In order to understand which factors contributed to such group differences, the baseline covariates such as ADASCOG13, mmseTOT (Mini-Mental State Examination total score), FAQTOTAL (functional activities questionnaires total score), cdrSB (clinical dementia rating sum of boxes), ApoE4 (Apolipoprotein E4) status and Education are summarized and differences between the two subgroups are tested in Table 5. ADASCOG13, mmseTOT, FAQTOTAL and cdrSB are the baseline cognitive or functional measurements. Since there are 8 patients missing their baseline information, we only consider 946 patients in the non-progression group and 297 patients in the progression group. As all the P-values are highly significant in Table 5, we could conclude that there are significant differences between the two subgroups. Compared with the non-progression group, the patients in the progression group has higher dementia severity in general based on higher ADASCOG13, FAQTOTAL, cdrSB and lower mmseTOT at baseline, more AopE4 carrier, and less education years. This could be validated with current literature. In general, the cognition tends to decrease more if the disease of the patient is more severe at baseline. ApoE4 was known as one important risk factor for AD onset and ApoE4 carriers tend to show earlier cognitive decline onset than the non-carriers (Safieh et al., 2019). In addition, some studies showed that patients with lower education were more likely to develop AD (Katzman, 1993). Therefore, our research could

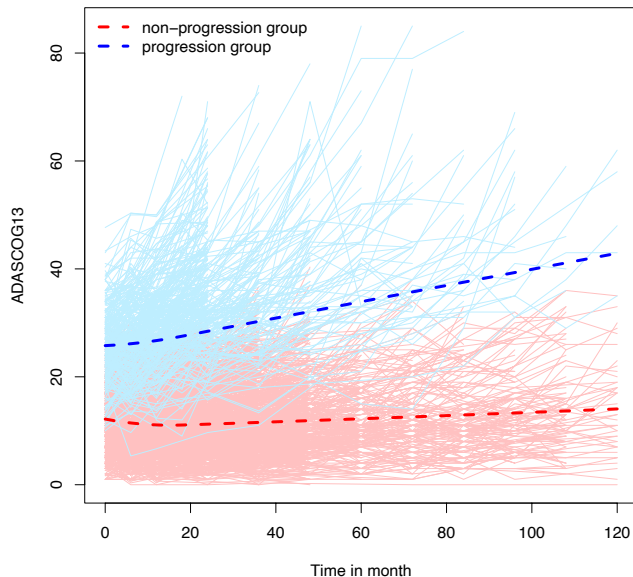


Fig. 6: The trajectories of the clustered subgroups (blue, red solid lines) and their corresponding fitted curves (dashed lines) based on ADASCOG13. The blue group is the progression group, with higher values of ADASCOG13 indicating faster cognition decline.

provide insight into trial entry criteria for AD.

Next, given the baseline covariates in Table 5, we made predictions on the clustered population. It should be noted that the ratio of patients in these two subgroups is $946 : 297 \approx 3.19 : 1$. We have class imbalance here, which could result in poor predictive performance for the minority class. To address this problem, we utilized sampling methods so that a balanced data set can be used. We focused on three approaches: over-sampling, down-sampling and synthetic minority over-sampling technique (SMOTE). Over-sampling is to resample the minority class randomly with replacement until it has the same number of objects as the majority class, while down-sampling is to delete

Baseline Covariates	Non-progression group (N=946)	Progression group (N=297)	P-value
	Mean (SD)	Mean (SD)	
ADASCOG13	12.16 (5.52)	25.79 (6.45)	< 0.001
mmseTOT	28.33 (1.70)	25.12 (2.49)	< 0.001
FAQTOTAL	1.59 (3.16)	8.48 (6.86)	< 0.001
cdrSB	0.87 (0.99)	2.89 (1.69)	< 0.001
ApoE4 carrier (%)	37% (0.02)	72% (0.03)	< 0.001
Education	16.17 (2.72)	15.32 (3.09)	< 0.001

Table 5: Mean and standard deviation (SD) for each baseline covariate; P-value shows the significant difference existing in the two subgroups. ApoE4 is tested by two proportion z-test, while other covariates are tested by two sample t-test.

some objects randomly from the majority class until it matches the size of the minority class. SMOTE, proposed by [Chawla et al. \(2002\)](#), is to create synthetic examples from the minority class instead of over-sampling with replacement. Then we compared the prediction results using four different predictive models: logistic regression, random forest, support vector machine (SVM) with linear kernel and boosting. To evaluate the prediction performance, we use precision, recall and F1 score. Precision measures the proportion of positive identifications that are actually correct, while recall is the proportion of actual positives that are identified correctly. F1 score is the weighted average between precision and recall. Here the progression group is defined as the positive class. As shown in Table 6, compared with original data set, precision under different predictive models using sampling methods (over-sampling, down-sampling and SMOTE) decreases, while recall increases. As recall measures the proportion of predicting the patients in progression group to the progression group and all the values are above 0.8, our predictive models would be useful to predict whether the patient should be enrolled in future AD clinical trials.

Predictive model	Performance	Sampling methods			
		Original	Over-sampling	Down-sampling	SMOTE
Logistic	Precision	0.836	0.689	0.686	0.692
	Recall	0.764	0.874	0.874	0.877
	F1 score	0.796	0.768	0.767	0.771
Random forest	Precision	0.828	0.785	0.692	0.753
	Recall	0.780	0.826	0.884	0.859
	F1 score	0.801	0.803	0.774	0.801
Boosting	Precision	0.833	0.730	0.714	0.718
	Recall	0.785	0.885	0.884	0.871
	F1 score	0.806	0.798	0.788	0.786
SVM	Precision	0.838	0.681	0.684	0.682
	Recall	0.749	0.870	0.877	0.870
	F1 score	0.790	0.762	0.767	0.762

Table 6: Precision, recall and F1 score of different predictive models based on different sampling methods under 10-fold cross-validation. The progression group is the positive class. “Original” under the sampling methods means using the original data instead of sampling data.

7 Discussion

In this paper, we consider the subgroup analysis for longitudinal trajectories of the AD data based on a heterogeneous nonparametric regression model. We use B-splines to approximate the non-parametric functional curves, and cluster the subjects into subgroups by applying concave pairwise fusion penalties on the spline coefficients. Our method can automatically identify the latent mem-

berships, and recover the disease trajectory curves of subgroups simultaneously without an prior knowledge of the number of the subgroups. Different from the GMM method that requires to specify an underlying distribution of the data, our method only needs a working correlation matrix of the repeated measures within each subject. Moreover, the resulting estimators of the functional curves are robust to the specification of the working correlation matrix. Simulation studies indicate promising performance of our proposed method. It has been demonstrated as an effective tool for subgroup analysis of the AD data considered in this paper. As a future work, we plan to extend the proposed method to the joint modeling of survival and longitudinal data, which commonly occur in clinical studies. However, further investigations are needed to develop the computational algorithm and theoretical properties.

8 Acknowledgement

Data used in preparation of this article were obtained from the Alzheimer’s Disease Neuroimaging Initiative (ADNI) database (adni.loni.usc.edu). As such, the investigators within the ADNI contributed to the design and implementation of ADNI and/or provided data but did not participate in analysis or writing of this report. A complete listing of ADNI investigators can be found at: http://adni.loni.usc.edu/wp-content/uploads/how_to_apply/ADNI_Acknowledgement_List.pdf.

The authors thank Xiang Zhang and Peter F. Castelluccio, former Eli Lilly and Company employees, for their help in data organization. Yushi Liu, Bochao Jia and Luna Sun are stockholders and employees of Eli Lilly and Company.

The research of Mingming Liu and Shujie Ma is supported in part by the U.S. NSF grants DMS-17-12558 and DMS-20-14221 and the UCR Academic Senate CoR Grant. Jing Yang’s research is supported by the National Natural Science Foundation of China (Grant 11801168), the Natural Science Foundation of Hunan Province (Grant 2018JJ3322), the Scientific Research Fund of Hunan Provincial Education Department (Grant 18B024), and the project of China Scholarship Council for his visiting to Professor Shujie Ma at University of California, Riverside.

Data collection and sharing for this project was funded by the Alzheimer’s Disease Neuroimaging Initiative (ADNI) (National Institutes of Health Grant U01 AG024904) and DOD ADNI (Depart-

ment of Defense award number W81XWH-12-2-0012). ADNI is funded by the National Institute on Aging, the National Institute of Biomedical Imaging and Bioengineering, and through generous contributions from the following: AbbVie, Alzheimer's Association; Alzheimer's Drug Discovery Foundation; Araclon Biotech; BioClinica, Inc.; Biogen; Bristol-Myers Squibb Company; CereSpir, Inc.; Cogstate; Eisai Inc.; Elan Pharmaceuticals, Inc.; Eli Lilly and Company; EuroImmun; F. Hoffmann-La Roche Ltd and its affiliated company Genentech, Inc.; Fujirebio; GE Healthcare; IXICO Ltd.; Janssen Alzheimer Immunotherapy Research & Development, LLC.; Johnson & Johnson Pharmaceutical Research & Development LLC.; Lumosity; Lundbeck; Merck & Co., Inc.; Meso Scale Diagnostics, LLC.; NeuroRx Research; Neurotrack Technologies; Novartis Pharmaceuticals Corporation; Pfizer Inc.; Piramal Imaging; Servier; Takeda Pharmaceutical Company; and Transition Therapeutics. The Canadian Institutes of Health Research is providing funds to support ADNI clinical sites in Canada. Private sector contributions are facilitated by the Foundation for the National Institutes of Health (<http://www.fnih.org>). The grantee organization is the Northern California Institute for Research and Education, and the study is coordinated by the Alzheimer's Therapeutic Research Institute at the University of Southern California. ADNI data are disseminated by the Laboratory for Neuro Imaging at the University of Southern California.

Appendix

A.1 Computation procedure using ADMM algorithm

It is worth noting that the penalty function in (3.3) is not separable in γ_i 's. Following Ma et al. (2019), we derive an ADMM algorithm to minimize the objective function (3.3). By introducing a new set of parameters $\delta_{ij} = \gamma_i - \gamma_j$, the problem can be reformulated as the following constrained optimization:

$$\begin{aligned} \min \quad & \frac{1}{2} \sum_{i=1}^n (\mathbf{Y}_i - \mathbf{X}_i \gamma_i)^T \mathbf{V}_i^{-1} (\mathbf{Y}_i - \mathbf{X}_i \gamma_i) + \sum_{1 \leq i < j \leq n} p_\tau (\|\delta_{ij}\|_2, \lambda), \\ \text{subject to} \quad & \gamma_i - \gamma_j - \delta_{ij} = \mathbf{0}, \end{aligned} \quad (\text{A.1})$$

Denote by $\langle \mathbf{a}, \mathbf{b} \rangle = \mathbf{a}^T \mathbf{b}$ the inner product of two vectors. The above constrained optimization can be transformed into its augmented Lagrangian optimization problem, i.e., minimize:

$$\begin{aligned} L(\gamma, \delta, \mathbf{v}) = & \frac{1}{2} \sum_{i=1}^n (\mathbf{Y}_i - \mathbf{X}_i \gamma_i)^T \mathbf{V}_i^{-1} (\mathbf{Y}_i - \mathbf{X}_i \gamma_i) + \sum_{1 \leq i < j \leq n} p_\tau (\|\delta_{ij}\|_2, \lambda) \\ & + \sum_{i < j} \langle \mathbf{v}_{ij}, \gamma_i - \gamma_j - \delta_{ij} \rangle + \frac{\vartheta}{2} \sum_{i < j} \|\gamma_i - \gamma_j - \delta_{ij}\|_2^2, \end{aligned} \quad (\text{A.2})$$

where $\delta = \{\delta_{ij}^T, i < j\}^T$, the dual variables $\mathbf{v} = \{\mathbf{v}_{ij}^T, i < j\}^T$ are the Lagrange multipliers and ϑ is the penalty parameter. Then we can compute the estimates of $(\gamma, \delta, \mathbf{v})$ through iterations using the ADMM algorithm.

Given the value of δ^m, \mathbf{v}^m at step m , we update the estimates at step $m+1$ as follows:

$$\gamma^{m+1} = \underset{\gamma}{\operatorname{argmin}} L(\gamma, \delta^m, \mathbf{v}^m), \quad (\text{A.3})$$

$$\delta^{m+1} = \underset{\delta}{\operatorname{argmin}} L(\gamma^{m+1}, \delta, \mathbf{v}^m), \quad (\text{A.4})$$

$$\mathbf{v}_{ij}^{m+1} = \mathbf{v}_{ij}^m + \vartheta (\gamma_i^{m+1} - \gamma_j^{m+1} - \delta_{ij}^{m+1}). \quad (\text{A.5})$$

Notice that the problem in (A.3) is equivalent to minimizing the function

$$\begin{aligned} f(\gamma) &= \frac{1}{2} \sum_{i=1}^n (\mathbf{Y}_i - \mathbf{X}_i \gamma_i)^T \mathbf{V}_i^{-1} (\mathbf{Y}_i - \mathbf{X}_i \gamma_i) + \frac{\vartheta}{2} \sum_{i < j} \|\gamma_i - \gamma_j - \delta_{ij}^m + \vartheta^{-1} \mathbf{v}_{ij}^m\|_2^2 + C_0 \\ &= \frac{1}{2} (\mathbf{Y} - \mathbf{X} \gamma)^T \mathbf{V}^{-1} (\mathbf{Y} - \mathbf{X} \gamma) + \frac{\vartheta}{2} \|\mathbf{A} \gamma - \delta^m + \vartheta^{-1} \mathbf{v}^m\|_2^2 + C_0, \end{aligned}$$

where $\mathbf{Y} = (\mathbf{Y}_1, \dots, \mathbf{Y}_n)^T$, $\mathbf{X} = \operatorname{diag}(\mathbf{X}_1, \dots, \mathbf{X}_n)$, $\mathbf{V} = \operatorname{diag}(\mathbf{V}_1, \dots, \mathbf{V}_n)$, $\mathbf{A} = \mathbf{D} \otimes \mathbf{I}_d$ (Kronecker product) and C_0 is a constant independent of γ . Here $\mathbf{D} = \{(\mathbf{e}_i - \mathbf{e}_j), i < j\}^T$, in which \mathbf{e}_i is a

$n \times 1$ vector with the i th element being 1 and the remaining ones being 0, and \mathbf{I}_d is a $d \times d$ identity matrix. Thus, we can update $\boldsymbol{\gamma}^{m+1}$ by:

$$\boldsymbol{\gamma}^{m+1} = (\mathbf{X}^T \mathbf{V}^{-1} \mathbf{X} + \vartheta \mathbf{A}^T \mathbf{A})^{-1} [\mathbf{X}^T \mathbf{V}^{-1} \mathbf{Y} + \vartheta \mathbf{A}^T (\boldsymbol{\delta}^m - \vartheta^{-1} \mathbf{v}^m)]. \quad (\text{A.6})$$

In (A.4), given $\boldsymbol{\gamma}^{m+1}$ and \mathbf{v}^m , the minimization problem is the same as minimizing

$$\frac{\vartheta}{2} \|\boldsymbol{\zeta}_{ij}^m - \boldsymbol{\delta}_{ij}\|_2^2 + p_\tau(\|\boldsymbol{\delta}_{ij}\|_2, \lambda)$$

with respect to $\boldsymbol{\delta}_{ij}$, where $\boldsymbol{\zeta}_{ij}^m = \boldsymbol{\gamma}_i^{m+1} - \boldsymbol{\gamma}_j^{m+1} + \vartheta^{-1} \mathbf{v}_{ij}^m$. Consequently, for MCP penalty with $\tau > 1/\vartheta$, we have:

$$\boldsymbol{\delta}_{ij}^{m+1} = \begin{cases} \frac{S(\boldsymbol{\zeta}_{ij}^m, \lambda/\vartheta)}{1-1/(\tau\vartheta)} & \text{if } \|\boldsymbol{\zeta}_{ij}^m\|_2 \leq \tau\lambda, \\ \boldsymbol{\zeta}_{ij}^m & \text{if } \|\boldsymbol{\zeta}_{ij}^m\|_2 > \tau\lambda, \end{cases} \quad (\text{A.7})$$

where $S(\mathbf{z}, t) = (1 - t/\|\mathbf{z}\|_2)_+ \mathbf{z}$ is the groupwise soft thresholding operator.

The detailed ADMM algorithm is summarized as follows:

Algorithm 1 ADMM algorithm

Initialize: $\boldsymbol{\delta}^0, \mathbf{v}^0$.

For $m = 0, 1, 2, \dots$ **compute** $\boldsymbol{\gamma}^{m+1}$ in (A.3), then $\boldsymbol{\delta}^{m+1}$ in (A.4), and \mathbf{v}^{m+1} in (A.5);

If convergence criterion is met, **then** stop and denote the last iteration by $\hat{\boldsymbol{\gamma}}$, **else** $m = m + 1$.

Here we stop the ADMM algorithm when the primal residual $\mathbf{r}^{m+1} = \mathbf{A}\boldsymbol{\gamma}^{m+1} - \boldsymbol{\delta}^{m+1}$ is close to zero such that $\|\mathbf{r}^{(m+1)}\|_2 < \varepsilon$ for some small value $\varepsilon > 0$.

A.1.1 Initial value for starting ADMM algorithm and computation of solution path

To start ADMM algorithm, an appropriate initial value is very important. First, given model (3.2), we use the ordinary least squares estimate of each subject as the initial estimate $\boldsymbol{\gamma}^0$, i.e. $\boldsymbol{\gamma}_i^0 = (\mathbf{X}_i^T \mathbf{X}_i)^{-1} \mathbf{X}_i^T \mathbf{Y}_i, i = 1, \dots, n$, which is a consistent estimate. Then, let initial estimates $\boldsymbol{\delta}_{ij}^0 = \boldsymbol{\gamma}_i^0 - \boldsymbol{\gamma}_j^0$ in $\boldsymbol{\delta}^0$ and $\mathbf{v}^0 = \mathbf{0}$.

In order to compute the solution path of $\boldsymbol{\gamma}$ against λ , we consider a grid of λ values with $\lambda_{\min} = \lambda_0 < \lambda_1 < \dots < \lambda_K = \lambda_{\max}$, where $0 \leq \lambda_{\min} < \lambda_{\max} < \infty$. Given a λ value in $[\lambda_{\min}, \lambda_{\max}]$, we can compute $\hat{\boldsymbol{\gamma}}(\lambda)$ given in (3.4) by using ADMM algorithm. Referring to Ma et al. (2019), a warm start and continuation strategy is used for updating the solutions. Specifically, we compute $\hat{\boldsymbol{\gamma}}(\lambda_0)$ by using $\boldsymbol{\gamma}^0$ as the initial value, then $\hat{\boldsymbol{\gamma}}(\lambda_k)$ by using $\hat{\boldsymbol{\gamma}}(\lambda_{k-1})$ as the initial value ($k = 1, \dots, K$).

A.2 Consistency and convergence

Let C denotes a generic constant that might assume different values at different places. Without loss of generality, we consider the following B-spline basis functions that span G , that is, $B_k = J_n^{1/2} S_k$, $k = 1, \dots, J_n$, where $\{S_k\}_{k=1}^{J_n}$ are the B-splines defined in Chapter 5 of [Lorentz and DeVore \(1993\)](#). It follows from Theorem 4.2 of [Lorentz and DeVore \(1993\)](#) that

$$M_1 \|\boldsymbol{\gamma}\|_2^2 \leq \int \left\{ \sum_{k=1}^{J_n} B_k(t) \gamma_k \right\}^2 dt \leq M_2 \|\boldsymbol{\gamma}\|_2^2 \quad (\text{A.8})$$

for some constants $0 < M_1 < M_2 < \infty$, where $\boldsymbol{\gamma} = (\gamma_1, \dots, \gamma_{J_n})^T$.

Lemma A.1 *For each i , there exist some constants $0 < M_1 < M_2 < \infty$ such that, except on an event whose probability tends to zero, all the eigenvalues of $\mathbf{X}_i^T \mathbf{X}_i / m_i$ fall between M_1 and M_2 .*

Lemma A.2 *Assume the random variables ξ and η be F_1^k -measurable and F_{k+s}^∞ -measurable, respectively. If $E(|\xi|^p) < \infty$, $E(|\eta|^q) < \infty$ for some $p, q > 1$ and $1/p + 1/q < 1$. Then, under α -mixing,*

$$|E(\xi\eta) - E(\xi)E(\eta)| \leq 10\alpha(s)^{1-\frac{1}{p}-\frac{1}{q}} \|\xi\|_p \|\eta\|_q,$$

where $\|\xi\|_p = E^{1/p}(|\xi|^p)$ denotes the L_p -norm of ξ .

The proof of Lemma A.1 and Lemma A.2 can be respectively referred to Lemma 2 of [Huang and Shen \(2004\)](#) and Theorem 7.3 of [Roussas and Ioannides \(1987\)](#).

Define $\beta_i^*(t) = \mathbf{B}(t)^T \boldsymbol{\gamma}^* \in G$ such that $\|\beta_i^*(t) - \beta_i(t)\|_2 = \inf_{g \in G} \|g(t) - \beta_i(t)\|_2 \triangleq \varpi_i$, it follows from the result on page 149 of [De Boor \(2001\)](#) that $\varpi_i = J_n^{-r}$ if $\beta_i \in \mathcal{H}_r$.

A.2.1 Consistency of initial estimator

Proposition A.1 *Under conditions (C1)-(C4), the initial estimators $\hat{\beta}_i^{(0)}$, $i = 1, \dots, n$, satisfy $\|\hat{\beta}_i^{(0)} - \beta_i\|_2^2 = O_p(J_n/m_i + J_n^{-2r})$.*

Proof. Recall that

$$\hat{\boldsymbol{\gamma}}_i^{(0)} = \arg \min_{\boldsymbol{\gamma}_i} (\mathbf{Y}_i - \mathbf{X}_i \boldsymbol{\gamma}_i)^T (\mathbf{Y}_i - \mathbf{X}_i \boldsymbol{\gamma}_i) = (\mathbf{X}_i^T \mathbf{X}_i)^{-1} \mathbf{X}_i^T \mathbf{Y}_i,$$

and $\hat{\beta}_i^{(0)}(t) = \mathbf{B}(t)^T \hat{\gamma}_i^{(0)}$. Now, define $\tilde{\gamma}_i^{(0)} = (\mathbf{X}_i^T \mathbf{X}_i)^{-1} \mathbf{X}_i^T \tilde{\mathbf{Y}}_i$, $\tilde{\beta}_i^{(0)}(t) = \mathbf{B}(t)^T \tilde{\gamma}_i^{(0)}$, where $\tilde{\mathbf{Y}}_i = (\beta_i(t_{i1}), \dots, \beta_i(t_{im_i}))^T$. Obviously,

$$\hat{\gamma}_i^{(0)} - \tilde{\gamma}_i^{(0)} = (\mathbf{X}_i^T \mathbf{X}_i)^{-1} \mathbf{X}_i^T (\mathbf{Y}_i - \tilde{\mathbf{Y}}_i) = (\mathbf{X}_i^T \mathbf{X}_i)^{-1} \mathbf{X}_i^T \boldsymbol{\varepsilon}_i,$$

where $\boldsymbol{\varepsilon}_i = (\varepsilon_{i1}, \dots, \varepsilon_{im_i})^T$. It follows from Lemma A.1 that there exists a constant $C > 0$, such that

$$E(\boldsymbol{\varepsilon}_i^T \mathbf{X}_i (\mathbf{X}_i^T \mathbf{X}_i)^{-1} (\mathbf{X}_i^T \mathbf{X}_i)^{-1} \mathbf{X}_i^T \boldsymbol{\varepsilon}_i) \leq C \frac{1}{m_i^2} E(\boldsymbol{\varepsilon}_i^T \mathbf{X}_i \mathbf{X}_i^T \boldsymbol{\varepsilon}_i).$$

Taking $p = q = 4$ in Lemma A.2 and by the properties of B-splines, we can obtain

$$\begin{aligned} E(\boldsymbol{\varepsilon}_i^T \mathbf{X}_i \mathbf{X}_i^T \boldsymbol{\varepsilon}_i) &= E \left\{ \sum_{k=1}^{J_n} \left(\sum_{j=1}^{m_i} B_k(t_{ij}) \varepsilon_{ij} \right)^2 \right\} = E \left\{ \sum_{j,j'=1}^{m_i} \sum_{k=1}^{J_n} \varepsilon_{ij} \varepsilon_{ij'} B_k(t_{ij}) B_k(t_{ij'}) \right\} \\ &\leq J_n \sum_{j,j'=1}^{m_i} |E(\varepsilon_{ij} \varepsilon_{ij'})| \leq 10 J_n \sum_{1 \leq j,j' \leq m_i} \alpha(|j-j'|)^{1/2} [E(|\varepsilon_{ij}|^4)]^{1/4} [E(|\varepsilon_{ij'}|^4)]^{1/4} \\ &= O_p(J_n m_i), \end{aligned}$$

where the last equality holds because $\sum_{s=1}^{\infty} \alpha(s)^{1/2} [E(|\varepsilon_{ij}|^4)]^{1/4} [E(|\varepsilon_{ij'}|^4)]^{1/4}$ is bounded from condition (C2). Thus, $\|\hat{\gamma}_i^{(0)} - \tilde{\gamma}_i^{(0)}\|_2^2 = O_p(J_n/m_i)$. This together with expression (A.8) leads to

$$\|\hat{\beta}_i^{(0)}(t) - \tilde{\beta}_i^{(0)}(t)\|_2^2 = O\left(\|\hat{\gamma}_i^{(0)} - \tilde{\gamma}_i^{(0)}\|_2^2\right) = O_p(J_n/m_i). \quad (\text{A.9})$$

On the other hand, by Lemma A.1, we have

$$\|\tilde{\gamma}_i^{(0)} - \gamma_i^*\|_2^2 = O_p\left(\frac{1}{m_i} (\tilde{\gamma}_i^{(0)} - \gamma_i^*)^T \mathbf{X}_i^T \mathbf{X}_i (\tilde{\gamma}_i^{(0)} - \gamma_i^*)\right).$$

Noting that $\mathbf{X}_i \tilde{\gamma}_i^{(0)} = \mathbf{X}_i (\mathbf{X}_i^T \mathbf{X}_i)^{-1} \mathbf{X}_i^T \tilde{\mathbf{Y}}_i$ is an orthogonal projection of $\tilde{\mathbf{Y}}_i$. Hence,

$$\begin{aligned} \frac{1}{m_i} (\tilde{\gamma}_i^{(0)} - \gamma_i^*)^T \mathbf{X}_i^T \mathbf{X}_i (\tilde{\gamma}_i^{(0)} - \gamma_i^*) &\leq \frac{1}{m_i} (\tilde{\mathbf{Y}}_i - \mathbf{X}_i \gamma_i^*)^T (\tilde{\mathbf{Y}}_i - \mathbf{X}_i \gamma_i^*) \\ &= \frac{1}{m_i} \sum_{j=1}^{m_i} (\beta_i(t_{ij}) - \beta_i^*(t_{ij}))^2 \\ &= O(\varpi_i^2), \end{aligned}$$

It follows from expression (A.8) that

$$\|\tilde{\beta}_i^{(0)}(t) - \beta_i^*(t)\|_2^2 = O\left(\|\tilde{\gamma}_i^{(0)} - \gamma_i^*\|_2^2\right) = O_p(\varpi_i^2). \quad (\text{A.10})$$

Therefore, by the definition of ϖ_i , equations (A.9)-(A.10) and the triangle inequality, we have

$$\begin{aligned}
& \|\hat{\beta}_i^{(0)}(t) - \beta_i(t)\|_2^2 \\
& \leq \|\hat{\beta}_i^{(0)}(t) - \tilde{\beta}_i^{(0)}(t)\|_2^2 + \|\tilde{\beta}_i^{(0)}(t) - \beta_i^*(t)\|_2^2 + \|\beta_i^*(t) - \beta_i(t)\|_2^2 \\
& = O_p(J_n/m_i) + O_p(\varpi_i^2) + O_p(\varpi_i^2) = O_p(J_n/m_i + J_n^{-2r}).
\end{aligned}$$

This completes the proof.

A.2.2 Convergence of ADMM

Proposition A.2 *Let $\mathbf{r}^{m+1} = \mathbf{A}\boldsymbol{\gamma}^{m+1} - \boldsymbol{\delta}^{m+1}$ and $\mathbf{s}^{m+1} = \vartheta \mathbf{A}^T(\boldsymbol{\delta}^{m+1} - \boldsymbol{\delta}^m)$ respectively be the primal residual and dual residual in the ADMM. Then, $\lim_{m \rightarrow \infty} \|\mathbf{r}^{m+1}\|_2^2 = 0$ and $\lim_{m \rightarrow \infty} \|\mathbf{s}^{m+1}\|_2^2 = 0$ hold for MCP penalty.*

Proof. Taking a careful examination of our constructed objective function $L(\boldsymbol{\gamma}, \boldsymbol{\delta}, \boldsymbol{\nu})$ with that of [Ma et al. \(2019\)](#), the conclusion $\lim_{m \rightarrow \infty} \|\mathbf{r}^{m+1}\|_2^2 = 0$ can be directly derived by a similar proof of proposition 1 in [Ma et al. \(2019\)](#). Recall that $\boldsymbol{\gamma}^{m+1}$ minimize $L(\boldsymbol{\gamma}, \boldsymbol{\delta}^m, \boldsymbol{\nu}^m)$ by definition, thus

$$\begin{aligned}
0 &= \left. \frac{\partial L(\boldsymbol{\gamma}, \boldsymbol{\delta}^m, \boldsymbol{\nu}^m)}{\partial \boldsymbol{\gamma}} \right|_{\boldsymbol{\gamma}=\boldsymbol{\gamma}^{m+1}} = \mathbf{X}^T \mathbf{V}^{-1}(\mathbf{X}\boldsymbol{\gamma}^{m+1} - \mathbf{Y}) + \mathbf{A}^T \{\boldsymbol{\nu}^m + \vartheta(\mathbf{A}\boldsymbol{\gamma}^{m+1} - \boldsymbol{\delta}^m)\} \\
&= \mathbf{X}^T \mathbf{V}^{-1}(\mathbf{X}\boldsymbol{\gamma}^{m+1} - \mathbf{Y}) + \mathbf{A}^T \{[\boldsymbol{\nu}^{m+1} - \vartheta(\mathbf{A}\boldsymbol{\gamma}^{m+1} - \boldsymbol{\delta}^{m+1})] + \vartheta(\mathbf{A}\boldsymbol{\gamma}^{m+1} - \boldsymbol{\delta}^m)\} \\
&= \mathbf{X}^T \mathbf{V}^{-1}(\mathbf{X}\boldsymbol{\gamma}^{m+1} - \mathbf{Y}) + \mathbf{A}^T \boldsymbol{\nu}^{m+1} + \vartheta \mathbf{A}^T(\boldsymbol{\delta}^{m+1} - \boldsymbol{\delta}^m),
\end{aligned}$$

which implies

$$\mathbf{s}^{m+1} = \vartheta \mathbf{A}^T(\boldsymbol{\delta}^{m+1} - \boldsymbol{\delta}^m) = -\{\mathbf{X}^T \mathbf{V}^{-1}(\mathbf{X}\boldsymbol{\gamma}^{m+1} - \mathbf{Y}) + \mathbf{A}^T \boldsymbol{\nu}^{m+1}\}.$$

In view of $\lim_{m \rightarrow \infty} \|\mathbf{r}^m\|_2^2 = \lim_{m \rightarrow \infty} \|\mathbf{A}\boldsymbol{\gamma}^m - \boldsymbol{\delta}^m\|_2^2 = 0$, we have

$$0 = \lim_{m \rightarrow \infty} \left. \frac{\partial L(\boldsymbol{\gamma}, \boldsymbol{\delta}^m, \boldsymbol{\nu}^m)}{\partial \boldsymbol{\gamma}} \right|_{\boldsymbol{\gamma}=\boldsymbol{\gamma}^{m+1}} = \lim_{m \rightarrow \infty} \{\mathbf{X}^T \mathbf{V}^{-1}(\mathbf{X}\boldsymbol{\gamma}^{m+1} - \mathbf{Y}) + \mathbf{A}^T \boldsymbol{\nu}^{m+1}\} = \lim_{m \rightarrow \infty} -\mathbf{s}^{m+1}.$$

Therefore, we obtain $\lim_{m \rightarrow \infty} \|\mathbf{s}^{m+1}\|_2^2 = 0$, this completes the proof.

A.3 Proof of the Theorems

To prove the main theoretical results in this article, we first present the following lemma which will be frequently used in the sequel. Let $\bar{\beta}_i = \mathbf{B}(t)^T \bar{\gamma}_i$, where

$$\bar{\gamma}_i = \arg \min_{\boldsymbol{\gamma}_i} (\mathbf{Y}_i - \mathbf{X}_i \boldsymbol{\gamma}_i)^T \mathbf{V}_i^{-1} (\mathbf{Y}_i - \mathbf{X}_i \boldsymbol{\gamma}_i) = (\mathbf{X}_i^T \mathbf{V}_i^{-1} \mathbf{X}_i)^{-1} \mathbf{X}_i^T \mathbf{V}_i^{-1} \mathbf{Y}_i. \quad (\text{A.11})$$

Lemma A.3 Under conditions (C1)-(C5), we have $\|\bar{\beta}_i - \beta_i\|_2^2 = O_p(J_n/m_i + J_n^{-2r})$, $i = 1, \dots, n$.

Proof. For $i = 1, \dots, n$, let $\tilde{\beta}_i = \mathbf{B}(t)^T \tilde{\gamma}_i$ and $\tilde{\gamma}_i = (\mathbf{X}_i^T \mathbf{V}_i^{-1} \mathbf{X}_i)^{-1} \mathbf{X}_i^T \mathbf{V}_i^{-1} \tilde{\mathbf{Y}}_i$, where $\tilde{\mathbf{Y}}_i$ is defined as above. Obviously, $\bar{\beta}_i - \tilde{\beta}_i = (\mathbf{X}_i^T \mathbf{V}_i^{-1} \mathbf{X}_i)^{-1} \mathbf{X}_i^T \mathbf{V}_i^{-1} \boldsymbol{\varepsilon}_i$. By Lemma A.1 and the bounded assumption on the eigenvalues of V , it is easy to verify that there exist two constants $0 < C_1 \leq C_2 < \infty$, such that

$$C_1 \frac{1}{m_i^2} E(\boldsymbol{\varepsilon}_i^T \mathbf{V}_i^{-1} \mathbf{X}_i \mathbf{X}_i^T \mathbf{V}_i^{-1} \boldsymbol{\varepsilon}_i) \leq E\left(\|\bar{\beta}_i - \tilde{\beta}_i\|_2^2\right) \leq C_2 \frac{1}{m_i^2} E(\boldsymbol{\varepsilon}_i^T \mathbf{V}_i^{-1} \mathbf{X}_i \mathbf{X}_i^T \mathbf{V}_i^{-1} \boldsymbol{\varepsilon}_i).$$

According to the operation properties of the trace and expectation, we have

$$\begin{aligned} E(\boldsymbol{\varepsilon}_i^T \boldsymbol{\Sigma}_i^{-1} \mathbf{X}_i \mathbf{X}_i^T \boldsymbol{\Sigma}_i^{-1} \boldsymbol{\varepsilon}_i) &= \text{trace}\{E(\boldsymbol{\varepsilon}_i^T \boldsymbol{\Sigma}_i^{-1} \mathbf{X}_i \mathbf{X}_i^T \boldsymbol{\Sigma}_i^{-1} \boldsymbol{\varepsilon}_i)\} = E(\text{trace}\{\mathbf{X}_i^T \boldsymbol{\Sigma}_i^{-1} \boldsymbol{\varepsilon}_i \boldsymbol{\varepsilon}_i^T \boldsymbol{\Sigma}_i^{-1} \mathbf{X}_i\}) \\ &= E(\text{trace}\{\mathbf{X}_i^T \mathbf{V}_i^{-1} \boldsymbol{\Sigma}_i \mathbf{V}_i^{-1} \mathbf{X}_i\}) = \text{trace}\{E(\mathbf{X}_i^T \mathbf{V}_i^{-1} \boldsymbol{\Sigma}_i \mathbf{V}_i^{-1} \mathbf{X}_i)\} \\ &= O_p(m_i J_n), \end{aligned}$$

where the last equality holds due to condition (C5) and Lemma A.1. Hence, we obtain

$$\|\bar{\beta}_i - \tilde{\beta}_i\|_2^2 = O_p(J_n/m_i). \quad (\text{A.12})$$

Furthermore, as $\mathbf{V}_i^{-1/2} \mathbf{X}_i (\mathbf{X}_i^T \mathbf{V}_i^{-1} \mathbf{X}_i)^{-1} \mathbf{X}_i^T \mathbf{V}_i^{-1} \tilde{\mathbf{Y}}_i$ is an orthogonal projection of $\mathbf{V}_i^{-1/2} \tilde{\mathbf{Y}}_i$, we have

$$\begin{aligned} &\frac{1}{m_i} (\tilde{\gamma}_i - \gamma_i^*)^T \mathbf{X}_i^T \mathbf{V}_i^{-1} \mathbf{X}_i (\tilde{\gamma}_i - \gamma_i^*) \\ &= \frac{1}{m_i} \left\{ (\mathbf{X}_i^T \mathbf{V}_i^{-1} \mathbf{X}_i)^{-1} \mathbf{X}_i^T \mathbf{V}_i^{-1} \tilde{\mathbf{Y}}_i - \tilde{\gamma}_i^* \right\}^T \mathbf{X}_i^T \mathbf{V}_i^{-1/2} \mathbf{V}_i^{-1/2} \mathbf{X}_i \left\{ (\mathbf{X}_i^T \mathbf{V}_i^{-1} \mathbf{X}_i)^{-1} \mathbf{X}_i^T \mathbf{V}_i^{-1} \tilde{\mathbf{Y}}_i - \tilde{\gamma}_i^* \right\} \\ &= \frac{1}{m_i} \|\mathbf{V}_i^{-1/2} \mathbf{X}_i (\mathbf{X}_i^T \mathbf{V}_i^{-1} \mathbf{X}_i)^{-1} \mathbf{X}_i^T \mathbf{V}_i^{-1} \tilde{\mathbf{Y}}_i - \mathbf{V}_i^{-1/2} \mathbf{X}_i \gamma_i^*\|_2^2 \\ &\leq \frac{1}{m_i} \|\mathbf{V}_i^{-1/2} \tilde{\mathbf{Y}}_i - \mathbf{V}_i^{-1/2} \mathbf{X}_i \gamma_i^*\|_2^2 = \frac{1}{m_i} (\tilde{\mathbf{Y}}_i - \mathbf{X}_i \gamma_i^*)^T \mathbf{V}_i^{-1} (\tilde{\mathbf{Y}}_i - \mathbf{X}_i \gamma_i^*) \\ &= O_p\left(\frac{1}{m_i} \|\tilde{\mathbf{Y}}_i - \mathbf{X}_i \gamma_i^*\|_2^2\right) = O_p(\|\beta_i - \beta_i^*\|_2^2) = O_p(\varpi_i^2), \end{aligned}$$

where the antepenult equality holds by the bounded assumption on the eigenvalues of V . Combining the expression (A.8), condition (C5) as well as Lemma A.1 leads to

$$\|\bar{\beta}_i - \beta_i^*\|_2^2 = O(\|\tilde{\gamma}_i - \gamma_i^*\|_2^2) = O_p\left(\frac{1}{m_i} (\tilde{\gamma}_i - \gamma_i^*)^T \mathbf{X}_i^T \boldsymbol{\Sigma}_i^{-1} \mathbf{X}_i (\tilde{\gamma}_i - \gamma_i^*)\right) = O_p(\varpi_i^2). \quad (\text{A.13})$$

Consequently, it follows from equations (A.12), (A.13) and the definition of ϖ_i that

$$\|\bar{\beta}_i - \beta_i\|_2^2 \leq \|\bar{\beta}_i - \tilde{\beta}_i\|_2^2 + \|\tilde{\beta}_i - \beta_i^*\|_2^2 + \|\beta_i^* - \beta_i\|_2^2 = O_p(J_n/m_i + \varpi_i^2) = O_p(J_n/m_i + J_n^{-2r}).$$

This finishes the proof.

Proof of Theorem 1. Notice that, it is equivalent to individually obtaining $\hat{\theta}_k = \arg \min_{\theta_k} (\mathbf{Y}_{(k)} - \mathbf{X}_{(k)}\theta_k)^T \mathbf{V}_{(k)} (\mathbf{Y}_{(k)} - \mathbf{X}_{(k)}\theta_k)$ and $\hat{\alpha}_k = \mathbf{X}_{(k)}\hat{\theta}_k$ for each $k = 1, \dots, K$, where the subscript $\mathbf{A}_{(k)}$ denotes the submatrix of \mathbf{A} that composed by the rows belong to the k th subgroup. According to Lemma A.3, we have

$$\|\hat{\alpha}_k - \alpha_k\|_2^2 = O_p(J_n/N_k + J_n^{-2r}) \leq O_p(J_n/N_0 + J_n^{-2r}),$$

where α_k is the true functions in the k th group. As a result,

$$\|\hat{\beta}^{or} - \boldsymbol{\alpha}\|_2^2 = \sum_{k=1}^K \|\hat{\alpha}_k - \alpha_k\|_2^2 = O_p(J_n/N_0 + J_n^{-2r})$$

for any fixed K . This completes the proof.

Proof of Theorem 2. We first prove $\|\hat{\beta} - \hat{\beta}^{or}\|_2^2 = O_p(J_n/m_{(n)} + J_n^{-2r})$. Let $\delta_n = J_n/m_{(n)} + J_n^{-2r}$, if one can show that for any $\omega > 0$, there exists a large enough constant $M > 0$ satisfying

$$P \left\{ \inf_{\|\mathbf{X}(\boldsymbol{\gamma} - \hat{\boldsymbol{\gamma}}^{or})\|_2^2 = M\delta_n} L_n(\boldsymbol{\gamma}) > L_n(\hat{\boldsymbol{\gamma}}^{or}) \right\} \geq 1 - \omega, \quad (\text{A.14})$$

which means a local minimizer of $L_n(\boldsymbol{\gamma})$ existed in the ball $\mathbb{B} = \{\boldsymbol{\gamma} : \|\mathbf{X}(\boldsymbol{\gamma} - \hat{\boldsymbol{\gamma}}^{or})\|_2^2 \leq M\delta_n\}$. Then, $\|\hat{\beta} - \hat{\beta}^{or}\|_2^2 = O_p(J_n/m_{(n)} + J_n^{-2r})$ can be proved.

Let $L_{n1} = \frac{1}{2}(\mathbf{Y} - \mathbf{X}\boldsymbol{\gamma})^T \mathbf{V}^{-1}(\mathbf{Y} - \mathbf{X}\boldsymbol{\gamma})$, thus $\bar{\boldsymbol{\gamma}} = (\bar{\gamma}_1^T, \dots, \bar{\gamma}_n^T)^T$ minimize L_{n1} , where $\bar{\gamma}_i$, $i = 1, \dots, n$ are defined in (A.11). Let $\bar{\boldsymbol{\beta}} = \mathbf{X}\bar{\boldsymbol{\gamma}}$, it follows from Lemma A.3 that $\|\bar{\boldsymbol{\beta}} - \boldsymbol{\beta}\|_2^2 = \sum_{i=1}^n \|\bar{\beta}_i - \beta_i\|_2^2 = O_p(J_n/m_{(n)} + J_n^{-2r})$ for any fixed n . Combining this result with Theorem 1 leads to

$$\|\bar{\boldsymbol{\beta}} - \hat{\beta}^{or}\|_2^2 \leq \|\bar{\boldsymbol{\beta}} - \boldsymbol{\beta}\|_2^2 + \|\hat{\beta}^{or} - \boldsymbol{\beta}\|_2^2 = O_p(J_n/m_{(n)} + J_n^{-2r}),$$

which is equivalent to

$$\|\mathbf{X}(\bar{\boldsymbol{\gamma}} - \hat{\boldsymbol{\gamma}}^{or})\|_2^2 \leq C_0\delta_n \quad (\text{A.15})$$

for some constant C_0 from expression (A.8). Moreover, for any $k \neq k'$,

$$\begin{aligned} \|\hat{\alpha}_k - \hat{\alpha}_{k'}\|_2 &= \|\hat{\alpha}_k - \alpha_k + \alpha_k - \hat{\alpha}_{k'} + \alpha_{k'} - \alpha_{k'}\|_2 \\ &\geq \|\alpha_k - \alpha_{k'}\|_2 - \|\hat{\alpha}_k - \alpha_k\|_2 - \|\hat{\alpha}_{k'} - \alpha_{k'}\|_2 \\ &\geq b - \|\hat{\alpha}_k - \alpha_k\|_2 - \|\hat{\alpha}_{k'} - \alpha_{k'}\|_2. \end{aligned}$$

Thus, we have $\|\hat{\alpha}_k - \hat{\alpha}_{k'}\|_2 \geq b$ for sufficiently large N_0 from Theorem 1. Accordingly, $\|\hat{\boldsymbol{\theta}}_k - \hat{\boldsymbol{\theta}}_{k'}\|_2 \geq Cb$ for some constant $C > 0$. Similarly, for any $i \in \mathcal{G}_k, j \in \mathcal{G}_{k'}, k \neq k'$, we can derive that $\|\gamma_i - \gamma_j\|_2 \geq Cb$ for any γ lies in the ball constraint \mathbb{B} and sufficiently large m_n .

In addition, as $P_\tau(\cdot, \lambda) \geq 0$ and $P_\tau(0, \lambda) = 0$, then

$$\begin{aligned} &L_n(\boldsymbol{\gamma}) - L_n(\hat{\boldsymbol{\gamma}}^{or}) \\ &\geq L_{n1}(\boldsymbol{\gamma}) - L_{n1}(\hat{\boldsymbol{\gamma}}^{or}) + \sum_{\substack{i \in \mathcal{G}_k, j \in \mathcal{G}_{k'} \\ k \neq k'}} \{P_\tau(\|\gamma_i - \gamma_j\|_2, \lambda)\} - \sum_{k \neq k'} P_\tau(\|\hat{\boldsymbol{\theta}}_k - \hat{\boldsymbol{\theta}}_{k'}\|_2, \lambda). \end{aligned}$$

As $\|\hat{\boldsymbol{\theta}}_k - \hat{\boldsymbol{\theta}}_{k'}\|_2 \geq Cb$ and $\|\gamma_i - \gamma_j\|_2 \geq Cb$ for any $i \in \mathcal{G}_k, j \in \mathcal{G}_{k'}, k \neq k'$ from previous arguments, it follows from the condition $Cb \geq \tau\lambda$ that

$$\sum_{\substack{i \in \mathcal{G}_k, j \in \mathcal{G}_{k'} \\ k \neq k'}} \{P_\tau(\|\gamma_i - \gamma_j\|_2, \lambda)\} = 0$$

and

$$\sum_{k \neq k'} P_\tau(\|\hat{\boldsymbol{\theta}}_k - \hat{\boldsymbol{\theta}}_{k'}\|_2, \lambda) = 0$$

Thus,

$$L_n(\boldsymbol{\gamma}) - L_n(\hat{\boldsymbol{\gamma}}^{or}) \geq L_{n1}(\boldsymbol{\gamma}) - L_{n1}(\hat{\boldsymbol{\gamma}}^{or}).$$

Further by the definition of $\bar{\boldsymbol{\gamma}}$ and (A.15), we have $L_{n1}(\boldsymbol{\gamma}) \geq L_{n1}(\hat{\boldsymbol{\gamma}}^{or})$ for any $\boldsymbol{\gamma}$ satisfying $\|\mathbf{X}(\boldsymbol{\gamma} - \hat{\boldsymbol{\gamma}}^{or})\|_2^2 = M\delta_n$ with sufficiently large M . Therefore, (A.14) is proved, which means

$$\|\hat{\boldsymbol{\beta}} - \hat{\boldsymbol{\beta}}^{or}\|_2^2 = O_p(J_n/m_{(n)} + J_n^{-2r}).$$

Combing this result with Theorem 1 yields

$$\|\hat{\boldsymbol{\beta}} - \boldsymbol{\beta}\|_2^2 \leq \|\hat{\boldsymbol{\beta}} - \hat{\boldsymbol{\beta}}^{or}\|_2^2 + \|\hat{\boldsymbol{\beta}}^{or} - \boldsymbol{\beta}\|_2^2 = O_p(J_n/m_{(n)} + J_n^{-2r}).$$

This completes the proof of Theorem 2.

Proof of Theorem 3. (i) For $i, j \in \mathcal{G}_k$, we have $\beta_i = \beta_j$. Then

$$\begin{aligned} \|\hat{\beta}_i - \hat{\beta}_j\|_2^2 &\leq \|\hat{\beta}_i - \beta_i\|_2^2 + \|\beta_i - \beta_j\|_2^2 + \|\hat{\beta}_j - \beta_j\|_2^2 \\ &\leq 2 \max_i \|\hat{\beta}_i - \beta_i\|_2^2 + 0 = O_p(J_n/m_{(n)} + J_n^{-2r}) \rightarrow 0 \end{aligned}$$

as $m_{(n)} \rightarrow \infty$, where the last equality holds from Theorem 2. This means $\hat{\beta}_i$ and $\hat{\beta}_j$ will fall into the same group with probability approaching to 1.

(ii) For any $i \in \mathcal{G}_k, j \in \mathcal{G}_{k'}, k \neq k'$, it follows from Theorem 2 that

$$\begin{aligned} \|\hat{\beta}_i - \hat{\beta}_j\|_2^2 &= \|\hat{\beta}_i - \beta_i + \beta_i - \beta_j + \beta_j - \hat{\beta}_j\|_2^2 \\ &\geq \min_{\substack{i \in \mathcal{G}_k, j \in \mathcal{G}_{k'} \\ k \neq k'}} \|\beta_i - \beta_j\|_2^2 - 2 \max_{1 \leq i \leq n} \|\hat{\beta}_i - \beta_i\|_2^2 \\ &= b^2 - O_p(J_n/m_{(n)} + J_n^{-2r}) \rightarrow b^2 > 0, \end{aligned}$$

which implies that $\hat{\beta}_i$ and $\hat{\beta}_j$ will fall into the different groups with probability approaching to 1. Therefore, the proof is completed by the combinations of conclusions (i) and (ii).

In what follows, let $a_n \asymp b_n$ mean that a_n/b_n and b_n/a_n are bounded for given sequences of positive numbers a_n and b_n . For a square integrable function g on \mathbb{T} , we define the norms $\|g\|^2 = E(g(t)^2)$ and $\|g\|_\infty = \sup_{t \in \mathbb{T}} |g(t)|$.

Proof of Theorem 4. We can conclude from the results of Theorems 1-3 that the proposed penalized estimators performs asymptotically equivalent to the oracle ones as m_n approaching to infinite. Thus, we only need to prove the asymptotic normalities of the oracle estimators $\hat{\beta}^{or}(t) = (\hat{\alpha}_1(t), \dots, \hat{\alpha}_K(t))^T = \mathbb{B}(t)\hat{\theta}$, where $\hat{\theta} = (\hat{\theta}_1^T, \dots, \hat{\theta}_K^T)^T$. To this end, we first show that

$$\text{Var}(\hat{\alpha}_k(t))^{-1/2} \{\hat{\alpha}_k(t) - E(\hat{\alpha}_k(t))\} \xrightarrow{d} N(0, 1), \quad k = 1, \dots, K. \quad (\text{A.16})$$

Recall that $\hat{\theta}_k = \arg \min_{\theta_k} (\mathbf{Y}_{(k)} - \mathbf{X}_{(k)}\theta_k)^T \mathbf{V}_{(k)} (\mathbf{Y}_{(k)} - \mathbf{X}_{(k)}\theta_k) = \left(\mathbf{X}_{(k)}^T \mathbf{V}_{(k)}^{-1} \mathbf{X}_{(k)} \right)^{-1} \mathbf{X}_{(k)}^T \mathbf{V}_{(k)}^{-1} \mathbf{Y}_{(k)}$ for $k = 1, \dots, K$. We only consider an fixed k here since other cases can be proved in the

same way. For any $t \in \mathbb{T}$, $\hat{\alpha}_k(t) = \mathbf{B}(t)^T \hat{\boldsymbol{\theta}}_k = \mathbf{B}(t)^T \left(\mathbf{X}_{(k)}^T \mathbf{V}_{(k)}^{-1} \mathbf{X}_{(k)} \right)^{-1} \mathbf{X}_{(k)}^T \mathbf{V}_{(k)}^{-1} \mathbf{Y}_{(k)}$, and $\mathbb{E}(\hat{\alpha}_k(t)) = \mathbf{B}(t)^T \left(\mathbf{X}_{(k)}^T \mathbf{V}_{(k)}^{-1} \mathbf{X}_{(k)} \right)^{-1} \mathbf{X}_{(k)}^T \mathbf{V}_{(k)}^{-1} \boldsymbol{\alpha}_k(t)$. Thus,

$$\begin{aligned} \hat{\alpha}_k(t) - \mathbb{E}(\hat{\alpha}_k(t)) &= \mathbf{B}(t)^T \left(\mathbf{X}_{(k)}^T \mathbf{V}_{(k)}^{-1} \mathbf{X}_{(k)} \right)^{-1} \mathbf{X}_{(k)}^T \mathbf{V}_{(k)}^{-1} \boldsymbol{\varepsilon}_{(k)} \\ &= \mathbf{B}(t)^T \left(\mathbf{X}_{(k)}^T \mathbf{V}_{(k)}^{-1} \mathbf{X}_{(k)} \right)^{-1} \mathbf{X}_{(k)}^T \mathbf{V}_{(k)}^{-1} \boldsymbol{\Sigma}_{(k)}^{1/2} \boldsymbol{\Sigma}_{(k)}^{-1/2} \boldsymbol{\varepsilon}_{(k)} \\ &\triangleq \mathbf{B}(t)^T \left(\mathbf{X}_{(k)}^T \mathbf{V}_{(k)}^{-1} \mathbf{X}_{(k)} \right)^{-1} \mathbf{Z}_{(k)}^T \mathbf{e}_{(k)}, \end{aligned}$$

where $\mathbf{Z}_{(k)} = \boldsymbol{\Sigma}_{(k)}^{1/2} \mathbf{V}_{(k)}^{-1} \mathbf{X}_{(k)}$ and $\mathbf{e}_{(k)} = \boldsymbol{\Sigma}_{(k)}^{-1/2} \boldsymbol{\varepsilon}_{(k)}$. Obviously, we have $\mathbb{E}(\mathbf{e}_{(k)}) = 0$ and $\text{Var}(\mathbf{e}_{(k)}) = \mathbf{I}$, which means that the elements $\{e_{(k)\iota}\}_{\iota=1}^{N_k}$ can be seen as independent random variables with zero mean and unit variance.

Denote $\mathbf{Z}_{(k)\iota}^{\iota}$ as a J_n -dimensional column vector comprised by the ι th row of $\mathbf{Z}_{(k)}$, it follows that

$$\hat{\alpha}_k(t) - \mathbb{E}(\hat{\alpha}_k(t)) = \sum_{\iota=1}^{N_k} \mathbf{B}(t)^T \left(\mathbf{X}_{(k)}^T \mathbf{V}_{(k)}^{-1} \mathbf{X}_{(k)} \right)^{-1} \mathbf{Z}_{(k)\iota}^{\iota} e_{(k)\iota} = \sum_{\iota=1}^{N_k} \phi_{(k)\iota} e_{(k)\iota}$$

and

$$\text{Var}(\hat{\alpha}_k(t)) = \sum_{\iota=1}^{N_k} \phi_{(k)\iota}^2,$$

where $\phi_{(k)\iota} = \mathbf{B}(t)^T \left(\mathbf{X}_{(k)}^T \mathbf{V}_{(k)}^{-1} \mathbf{X}_{(k)} \right)^{-1} \mathbf{Z}_{(k)\iota}^{\iota}$. Therefore, if the Lindeberg condition holds, that is, $\max_{\iota} \phi_{(k)\iota}^2 / \sum_{\iota=1}^{N_k} \phi_{(k)\iota}^2 \rightarrow 0$, we can obtain that

$$\frac{\sum_{\iota=1}^{N_k} \phi_{(k)\iota} e_{(k)\iota}}{\sqrt{\sum_{\iota=1}^{N_k} \phi_{(k)\iota}^2}} \xrightarrow{d} N(0, 1), \quad (\text{A.17})$$

which indicates the result (A.16).

In fact, by the definition of $\mathbf{Z}_{(k)}$, condition (C5) and Lemma A.1, we have

$$\begin{aligned} \phi_{(k)\iota}^2 &= \left(\mathbf{B}(t)^T \left(\mathbf{X}_{(k)}^T \mathbf{V}_{(k)}^{-1} \mathbf{X}_{(k)} \right)^{-1} \mathbf{Z}_{(k)\iota}^{\iota} \right)^2 \asymp \frac{1}{N_k^2} \left(\mathbf{B}(t)^T \mathbf{Z}_{(k)\iota}^{\iota} \right)^2 \\ &\leq \frac{C}{N_k^2} \sum_{l=1}^{J_n} B_l^2(t) \sum_{l=1}^{J_n} B_l^2(t_{(k)\iota}), \end{aligned} \quad (\text{A.18})$$

where the last step holds by the Cauchy-Schwarz inequality and condition (C5). Moreover, based

on the same rationale as above, it follows that

$$\begin{aligned}
\sum_{\iota=1}^{N_k} \phi_{(k)\iota}^2 &= \mathbf{B}(t)^T \left(\mathbf{X}_{(k)}^T \mathbf{V}_{(k)}^{-1} \mathbf{X}_{(k)} \right)^{-1} \sum_{\iota=1}^{N_k} \mathbf{Z}_{(k)\iota}^{\iota} \mathbf{Z}_{(k)\iota}^T \left(\mathbf{X}_{(k)}^T \mathbf{V}_{(k)}^{-1} \mathbf{X}_{(k)} \right)^{-1} \mathbf{B}(t) \\
&= \mathbf{B}(t)^T \left(\mathbf{X}_{(k)}^T \mathbf{V}_{(k)}^{-1} \mathbf{X}_{(k)} \right)^{-1} \left(\mathbf{X}_{(k)}^T \mathbf{V}_{(k)}^{-1} \boldsymbol{\Sigma}_{(k)} \mathbf{V}_{(k)}^{-1} \mathbf{X}_{(k)} \right) \left(\mathbf{X}_{(k)}^T \mathbf{V}_{(k)}^{-1} \mathbf{X}_{(k)} \right)^{-1} \mathbf{B}(t) \\
&\asymp \mathbf{B}(t)^T \left(\mathbf{X}_{(k)}^T \mathbf{V}_{(k)}^{-1} \mathbf{X}_{(k)} \right)^{-1} \mathbf{B}(t) \asymp \frac{1}{N_k} \sum_{l=1}^{J_n} B_l^2(t). \tag{A.19}
\end{aligned}$$

Combining the expressions (A.18) and (A.19) leads to

$$\frac{\phi_{(k)\iota}^2}{\sum_{\iota=1}^{N_k} \phi_{(k)\iota}^2} \leq \frac{C}{N_k} \sum_{l=1}^{J_n} B_l^2(t_{(k)\iota}) \leq \frac{C}{N_k} \sup_{t \in \mathbb{T}} \sum_{l=1}^{J_n} B_l^2(t).$$

Observing that

$$\sup_{t \in \mathbb{T}} \sqrt{\sum_{l=1}^{J_n} B_l^2(t)} = \sup_{t \in \mathbb{T}} \sup_{b_l} \frac{\sum_{l=1}^{J_n} |B_l(t) b_l|}{\sqrt{\sum_{l=1}^{J_n} b_l^2}} \leq \sup_{b_l} \frac{\sup_{t \in \mathbb{T}} \sum_{l=1}^{J_n} |B_l(t) b_l|}{\sqrt{\sum_{l=1}^{J_n} b_l^2}} = \sup_{g \in G} \frac{\|g\|_{\infty}}{\|g\|_2},$$

where the last step due to expression (A.8). Based on the definitions of norms and condition (C1)

that the density function $f(t)$ is uniformly bounded away from 0 and infinity on \mathbb{T} , it easy to verify

$\|g\|_2 \asymp \|g\|$. Let $A_n = \sup_{g \in G} \|g\|_{\infty} / \|g\|$, hence

$$\max_{\iota} \frac{\phi_{(k)\iota}^2}{\sum_{\iota=1}^{N_k} \phi_{(k)\iota}^2} \leq \frac{C}{N_k} \sup_{g \in G} \frac{\|g\|_{\infty}^2}{\|g\|_2^2} \leq \frac{C}{N_k} \sup_{g \in G} \frac{\|g\|_{\infty}^2}{\|g\|^2} (1 + o_p(1)) = \frac{C A_n^2}{N_k} (1 + o_p(1)).$$

Based on conditions (C1) and (C4), we have $A_n^2 \asymp J_n$. Therefore,

$$\max_{\iota} \frac{\phi_{(k)\iota}^2}{\sum_{\iota=1}^{N_k} \phi_{(k)\iota}^2} \leq \frac{C A_n^2}{N_k} (1 + o_p(1)) \asymp \frac{J_n}{N_k} (1 + o_p(1)) \rightarrow 0,$$

which implies the validation of Lindeberg condition. Consequently, (A.17) is proved, and then

(A.16) holds.

On the other hand, according to conditions (C3) and (C4), it is easy to verify that all the conditions assumed in Theorem 5.1 of Huang (2003) hold. This implies, by virtue of condition (C5), that

$$|\mathbb{E}(\hat{\alpha}_k(t)) - \alpha_k(t)| = O_p(J_n^{-r}).$$

Moreover, it follows from (A.19), condition (C5), Lemma A.1 and the properties of B-spline that

$$\begin{aligned}
\text{Var}(\hat{\alpha}_k(t)) &= \mathbf{B}(t)^T \left(\mathbf{X}_{(k)}^T \mathbf{V}_{(k)}^{-1} \mathbf{X}_{(k)} \right)^{-1} \left(\mathbf{X}_{(k)}^T \mathbf{V}_{(k)}^{-1} \boldsymbol{\Sigma}_{(k)} \mathbf{V}_{(k)}^{-1} \mathbf{X}_{(k)} \right) \left(\mathbf{X}_{(k)}^T \mathbf{V}_{(k)}^{-1} \mathbf{X}_{(k)} \right)^{-1} \mathbf{B}(t) \\
&\asymp J_n / N_k.
\end{aligned}$$

Taking into account of $J_n/m_{(n)}^{1/(2r+1)} \rightarrow \infty$, we have

$$\sup_{t \in \mathbb{T}} \left| \frac{\mathbb{E}(\hat{\alpha}_k(t)) - \hat{\alpha}_k(t)}{\sqrt{\text{Var}(\hat{\alpha}_k(t))}} \right| = o_p(1). \quad (\text{A.20})$$

Combining the results of (A.16) and (A.20) leads to

$$\text{Var}(\hat{\alpha}_k(t))^{-1/2} (\hat{\alpha}_k(t) - \alpha_k(t)) \xrightarrow{d} N(0, 1). \quad (\text{A.21})$$

Finally, by the expression of $\hat{\boldsymbol{\beta}}^{or}(t)$ and the independence assumption of different subgroup, we can obtain

$$\text{Var}(\hat{\boldsymbol{\beta}}^{or}(t))^{-1/2} (\hat{\boldsymbol{\beta}}^{or}(t) - \boldsymbol{\alpha}(t)) \xrightarrow{d} N(\mathbf{0}, \mathbf{I}_K),$$

where

$$\text{Var}(\hat{\boldsymbol{\beta}}^{or}(t)) = \mathbb{B}(t) (\mathbf{X}^T \mathbf{V}^{-1} \mathbf{X})^{-1} (\mathbf{X}^T \mathbf{V}^{-1} \boldsymbol{\Sigma} \mathbf{V}^{-1} \mathbf{X}) (\mathbf{X}^T \mathbf{V}^{-1} \mathbf{X})^{-1} \mathbb{B}(t)^T.$$

Therefore, we complete the proof of Theorem 4 based on (A.21) and the conclusions of Theorems 1-3.

References

- Boyd, S., Parikh, N. and Chu, E. (2011). *Distributed optimization and statistical learning via the alternating direction method of multipliers*, Now Publishers Inc.
- Caliński, T. and Harabasz, J. (1974). A dendrite method for cluster analysis, *Communications in Statistics-Theory and Methods* **3**(1): 1–27.
- Chawla, N. V., Bowyer, K. W., Hall, L. O. and Kegelmeyer, W. P. (2002). Smote: synthetic minority over-sampling technique, *Journal of Artificial Intelligence Research* **16**: 321–357.
- De Boor, C. (2001). *A practical guide to splines*, Revised Edition. Springer, New York.
- Fraley, C. and Raftery, A. E. (2002). Model-based clustering, discriminant analysis, and density estimation, *Journal of the American Statistical Association* **97**(458): 611–631.
- Hartigan, J. A. and Wong, M. A. (1979). Algorithm as 136: A k-means clustering algorithm, *Journal of the Royal Statistical Society. Series C (Applied Statistics)* **28**(1): 100–108.
- Huang, J. Z. (2003). Local asymptotics for polynomial spline regression, *The Annals of Statistics* **31**(5): 1600–1635.
- Huang, J. Z. and Shen, H. (2004). Functional coefficient regression models for non-linear time series: a polynomial spline approach, *Scandinavian Journal of Statistics* **31**(4): 515–534.
- Jung, T. and Wickrama, K. A. S. (2008). An introduction to latent class growth analysis and growth mixture modeling, *Social and Personality Psychology Compass* **2**(1): 302–317.
- Katzman, R. (1993). Education and the prevalence of dementia and alzheimer’s disease, *Neurology* **43**(1): 13–20.
- Liang, K. Y. and Zeger, S. (1986). Longitudinal data analysis using generalized linear models, *Biometrika* **73**(1): 13–22.
- Liu, R. and Yang, L. (2010). Spline-backfitted kernel smoothing of additive coefficient model, *Econometric Theory* **26**(1): 29–59.

- Lorentz, G. and DeVore, R. (1993). *Constructive Approximation, Polynomials and Splines Approximation*, Springer-Verlag, New York, Berlin, Heidelberg.
- Ma, S. (2012). Two-step spline estimating equations for generalized additive partially linear models with large cluster sizes, *The Annals of Statistics* **40**(6): 2943–2972.
- Ma, S. (2014). A plug-in the number of knots selector for polynomial spline regression, *Journal of Nonparametric Statistics* **26**(3): 489–507.
- Ma, S. and Huang, J. (2017). A concave pairwise fusion approach to subgroup analysis, *Journal of the American Statistical Association* **112**(517): 410–423.
- Ma, S., Huang, J., Zhang, Z. and Liu, M. (2019). Exploration of heterogeneous treatment effects via concave fusion, *The International Journal of Biostatistics* **16**(1).
- Ma, S., Song, Q. and Wang, L. (2013). Simultaneous variable selection and estimation in semiparametric modeling of longitudinal/clustered data, *Bernoulli* **19**(1): 252–274.
- MacKinnon, J. G. and White, H. (1985). Some heteroskedasticity-consistent covariance matrix estimators with improved finite sample properties, *Journal of Econometrics* **29**(3): 305–325.
- McNicholas, P. D. (2010). Model-based classification using latent gaussian mixture models, *Journal of Statistical Planning and Inference* **140**(5): 1175–1181.
- Rand, W. M. (1971). Objective criteria for the evaluation of clustering methods, *Journal of the American Statistical Association* **66**(336): 846–850.
- Roussas, G. G. and Ioannides, D. (1987). Moment inequalities for mixing sequences of random variables, *Stochastic Analysis and Applications* **5**(1): 60–120.
- Safieh, M., Korczyn, A. D. and Michaelson, D. M. (2019). Apoe4: an emerging therapeutic target for alzheimer?s disease, *BMC Medicine* **17**(1): 1–17.
- Song, J. J., Lee, H. J., Morris, J. S. and Kang, S. (2007). Clustering of time-course gene expression data using functional data analysis, *Computational biology and chemistry* **31**(4): 265–274.

- Tibshirani, R. (1996). Regression shrinkage and selection via the lasso, *Journal of the Royal Statistical Society: Series B (Methodological)* **58**(1): 267–288.
- Vinh, N. X., Epps, J. and Bailey, J. (2010). Information theoretic measures for clusterings comparison: Variants, properties, normalization and correction for chance, *The Journal of Machine Learning Research* **11**: 2837–2854.
- Wang, N., Carroll, R. J. and Lin, X. (2005). Efficient semiparametric marginal estimation for longitudinal/clustered data, *Journal of the American Statistical Association* **100**(469): 147–157.
- Xue, L. and Liang, h. (2013). Polynomial spline estimation for a generalized additive coefficient model, *Scandinavian Journal of Statistics* **19**(1): 252–274.
- Yiannopoulou, K. G., Anastasiou, A. I., Zachariou, V. and Pelidou, S. H. (2019). Reasons for failed trials of disease-modifying treatments for alzheimer disease and their contribution in recent research, *Biomedicines* **7**(4): 97.
- Zhang, C. H. (2010). Nearly unbiased variable selection under minimax concave penalty, *The Annals of Statistics* **38**(2): 894–942.